I give permission for public access to my thesis and for copying to be done at the discretion of the archives' librarian and/or the College library.

_____ _____

Signature Date

The role of Aur-A in *Drosophila melanogaster* fat body remodeling

By

Danielle Arshinoff

A Paper Presented to the

Faculty of Mount Holyoke College in

Partial Fulfillment for the Requirements for

The Degree of Bachelor of Arts with

Honor

Program in Biochemistry

Mount Holyoke College

South Hadley, MA 01075

May 2017

This paper was prepared

under the direction of

Professor Craig Woodard

for eight credits.

ACKNOWLEDGEMENTS

I am grateful for this research experience and for all the support I have received. I would not have been able to perform this research without the help and support of multiple individuals during my time in the Woodard lab. First I would like to thank Professor Woodard, who has been my thesis advisor for the past three semesters. Not only did he introduce me to genetics and research but he has also been a huge influence on my Mount Holyoke College education.

I would also like to thank Blanca Carbajal Gonzalez who has not only instructed me on microscopy equipment and advised me on staining and imaging protocols, but was always ready to answer any questions I had. Without her, my images would not have been as clear as they are.

Dr. Arash Bashirullah, from the University of Wisconsin, donated the randomly mutated *Drosophila melanogaster* lines as well as the mapping lines. I would like to thank him for his generosity without which this genetic screen could not have been performed. I would also like to thank the flies for their sacrifices and patience while I was trying to determine their problems and mutated genes.

Professor Amy Camp and Professor Kerstin Nordstrom have been very supportive and I would like to thank each of them for agreeing to serve on my thesis committee. Professor Camp first introduced me to fluorescence microscopy in cell biology lab and Professor Nordstrom has inspired me with her passion for science.

I would also like to thank my fellow members of The Screen Team who have aided me in my research. I appreciate their company and emotional support especially when we were searching for a “bold notum”. I would also like to thank my friends who have listened to my speeches about the lovely flies. I appreciate their support, encouragement and wisdom.

Finally, I would like to thank the Biochemistry Program that funded my research during my time at Mount Holyoke College.

TABLE OF CONTENTS

LIST OF FIGURES

Page

LIST OF TABLES

Page

LIST OF EQUATIONS

Page

ABSTRACT

Tissue remodeling is an important process in multicellular organisms that is necessary for processes such as wound healing and tumor metastasis. For remodeling to occur, connective proteins of the extracellular matrix (ECM) must be cleaved so that cells can migrate. The migration of cells in wound healing promotes wound closure and ECM degradation allows cancerous cells to separate from the tumor to metastasize.

Drosophila melanogaster undergoes metamorphosis from larva to adult. Most larval tissues undergo apoptosis, but the larval fat body undergoes remodeling and persists until after the adult has eclosed. During remodeling, the larval fat body cells change from being polygonal cells connected in sheets to spherical cells that are free floating. Since *D. melanogaster* possess multiple tools for genetic analysis, this organism is a commonly used model organism in biomedical research.

Drosophila were fed EMS to establish mutations on their third chromosome and were then scored for lethality. Twenty of these lines are pharate adult lethal, wherein the newly formed adult flies fail to eclose from their pupal case, and have larval fat body remodeling abnormalities. The fat body phenotype was screened and categorized according to the level of remodeling. The chromosomal location of four of the mutated genes that cause pharate adult lethality and abnormal fat body remodeling was attempted to be established.

Three of the mutated lines were determined to have mutations in the *aur-A* gene. This gene is known to affect the cytoskeleton arrangement in neuroblasts, but its role in fat body remodeling is unknown. The results from this study suggest that that this mutated gene does affect the actin filament organization.

INTRODUCTION

Tissue Remodeling:

Tissue remodeling is an important process in multicellular organisms that is used in wound healing and metastasis. Tissue remodeling refers to the dynamic reconstruction of the tissue by connective protein degradation, allowing the proteins to rearrange in a new conformation. Remodeling can result in either normal reconstruction or the development of a pathogenic structure due to alternate modeling (Kuman *et al.*, 2014). Tissue remodeling is vital since tissues continually change depending on growth, an increase in mass (causing structural changes), and other physical or chemical signals including the environment in which an injury occurs. Tumor metastasis uses the process of remodeling to cleave a group of cells from the original tumor mass to allow these cells to travel in the blood to other tissues and create secondary tumor sites. The extra cellular matrix (ECM) needs to be degraded in order to allow the cleaved group of cells to migrate (Cox & Erler, 2011).

Tissues are composed of multiple cells connected by proteins of the extracellular matrix (ECM). The connective proteins in the basement membrane and cell-cell junctions and must be cleaved in order for cells to migrate (Jia *et al.*, 2014). The migration of cells in wound healing promote wound closure and allows cancerous cells to separate from the tumor and travel to another area of the body to create a metastasis (Smirnova *et al.*, 2016; Son & Harijan, 2014). These

connective proteins are cut with multiple matrix metalloproteinases (MMPs) that are specific for the type of connective protein. Various MMPs are necessary because different tissues contain distinct connective proteins (Tiede *et al.*, 2016). For example, bones contain collagen and bone minerals in their ECM but the ECM of blood is blood plasma. Mammalian tissues can be categorized into four groups: connective, epithelial, muscle and nerve. Cartilage, tendons, ligaments, bone matrix, skin, adipose tissue, blood and lymph, the connective tissues responsible for providing structure and body shape, all belong to the first category (Cowin, 2004).

Remodeling is also necessary for proper wound healing since it allows for the removal of dead cells, the reorganization of cells, and the connection between the two edges of split tissue. The process of wound healing can be divided into three distinct phases: inflammation, proliferation and remodeling. In the inflammation stage, a hemostatic cascade is induced to allow the formation of fibrin clots that later promote the migration of cells that participate in wound healing. The second stage is the proliferation stage, during which the fibrin is replaced with stronger collagen fibers that give the scar an inflexible quality. After this initial step is complete, the keratinocytes perform an inward epithelialization in the wound margin. The second stage ends at day 10-12 with wound contraction but this can take longer depending on the severity of the wound. The final stage, remodeling, beginning three weeks post injury is of primary interest. Remodeling can continue until six months after injury, when

collagen production and degradation is constant in the mature wound matrix. This allows the formation of tension lines in a tissue between cells. Cells that do not participate in remodeling undergo programmed cell death, which concludes the healing process (Son & Harijan, 2014).

The remodeling stage of mammalian wound healing is similar to the process of larval fat body remodeling in *Drosophila melanogaster* because the degradation of the ECM is used to reorganize cells in order to either form tension lines in wound healing or to form free floating cells in fat body remodeling. Due to the genetic similarity between *D. melanogaster* and humans, determining the biochemical pathway of larval fat body remodeling in *D. melanogaster* could elucidate the homologous pathway in humans. Once the remodeling pathway in wound healing is determined, advances in wound care can be made and the mechanism of metastasis can be elucidated in humans. 90% of cancer deaths are due to metastasis so gaining insight into the remodeling mechanism would also allow improvements in metastasis prevention and therefor in cancer survival (Cox & Erler, 2011). Tissue remodeling is involved in a variety of other diseases such as asthma and pulmonary hypertension (Tiede *et al.*, 2016). To develop better medical treatments, it is necessary to gain a better understanding of the tissue remodeling process. *Drosophila melanogaster*, whose fat body undergoes remodeling, is an exemplary model organism in which to study this process.

***Drosophila melanogaster*:**

Drosophila melanogaster has been used as a model organism for over a hundred years to study a variety of biological processes including embryonic development, aging, learning behavior, and genetics and inheritance. Since the first documented use of this model organism by William Castle at Harvard in 1901, the *Drosophila melanogaster* genome sequence has been determined and made available (Jennings, 2011). The size of the genome is approximately 180 Mb including approximately 13,600 genes. *D. melanogaster* possesses only four chromosomes: two large autosomes and XY sex chromosomes (Adams *et al.*, 2000).

Despite the differences between *D. melanogaster* and humans, 75% of human genes have homologs in the genome of *Drosophila melanogaster* and many of the biological mechanisms and processes controlling development and survival are conserved (Jennings, 2011). For this reason, the fruit fly is a commonly used model organism in medical research into human diseases. *Drosophila melanogaster* is easy to culture in the laboratory, produces large numbers of progeny, has a short life cycle and can be genetically altered using a variety of methods. Female fruit flies can lay up to 100 eggs over a period of 20 days. These eggs develop into fertile adults within 10 days at 25˚C (Jennings, 2011). The short life cycle of *D. melanogaster* allows for the quick completion of experiments that would take months or years in vertebrates. The use of RNAi, GFP fusion proteins and the UAS-GAL-4 system have been thoroughly studied in

D. melanogaster and allow for easy genetic manipulation (Jennings, 2011). Using these tools, the creation of transgenic and mutated fly lines resulting in the activation or inhibition of certain genes is simple. Some of these mutations result in "markers" that have a clearly visible phenotype that can then be scored (Hoskins *et al*., 2001). Dominant markers allow screening and a faster method of mapping the chromosomal position of an unknown gene (Sapiro *et al.*, 2013). Studying these processes in humans is complicated for moral, ethical and biological reasons but can be avoided when using *D. melanogaster*, invertebrates with no animal licensing laws and fewer ethical and safety issues. *Drosophila melanogaster* are also easy to keep in a laboratory setting and are inexpensive (Jennings, 2011).

The Life Cycle of *Drosophila melanogaster*:

The larval fat body remodeling process occurs during metamorphosis when the larva turns into an adult fly. In order to comprehend this transition, it is necessary to have an understanding of the entire *D. melanogaster* life cycle as seen in Figure 1. *D. melanogaster* has four major stages of development: embryo, larva, pupa and adult. However, within the larval stage there are three separate stages: the 1st, 2nd and 3rd instars (Weigmann *et al.*, 2003).

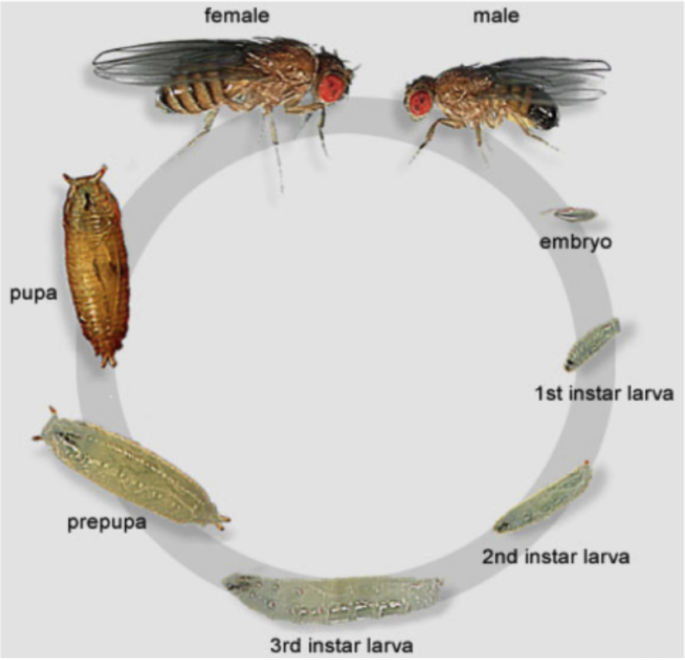

Figure 1: The different stages in the life cycle of *Drosophila melanogaster*. This organism starts as an embryo that develops into first a 1st instar larva, then a 2nd instar larva, and then 3rd instar larva that transforms into a prepupa. The prepupa stage marks the start of metamorphosis at approximately 120 hours from the start of development. From a prepupa the organism changes into a pupa and then an adult fly (Weigmann *et al*., 2003).

The life cycle of *D. melanogaster* requires around two weeks to complete at 25˚C. Once the egg has been fertilized, it requires one day to complete nuclear cleavage, gastrulation and organogenesis before it hatches to become a first instar larva. The first and second instar larval stages each require one day to be completed (National Research Council, 2000). At the end of each of these stages a molt occurs, during which the larva stops feeding and is motionless as the mouth hooks bite through the old cuticle. Next, the muscle contractions help rupture the old cuticle which is then discarded with the mouthparts and spiracles of the

previous developmental period. These three parts are reformed in the following instar larval stage (Riddiford & Truman, 1993). The third instar larval phase requires twice the amount of time (two days) and leads into the transition to a prepupa (Riddiford & Truman, 1993). The first two instars are buried in the food and use their mouth hooks to feed themselves. The larva continues to eat until a critical weight has been achieved, meaning the organism has reached a large enough size that will allow pupariation and maturation to occur. The main goal of the larval stage is to acquire enough nutrients to support morphogenesis, a process that requires a vast amount of energy when the organism is unable to feed. Towards the end of the larval stage of development, the late third instar larva wanders and climbs out of the food preparing to pupate. The larva wanders between 12 and 24 hours before puparium formation and then sticks to the side of the bottle (Riddiford & Truman, 1993; Tyler, 2000) In this position, the larva becomes motionless and its body shortens. The cuticle converts into the puparium, which initially appears white and soft but later hardens and turns brown (Tyler, 2000). At zero hours after puparium formation (APF), the puparium is still white and soft but the organism is motionless. This distinct appearance in development is used as a reference point for later developmental events (Riddiford & Truman, 1993). Inside the puparium the larva detaches as it molts for the last time to start metamorphosis at approximately 120 hours after the start of development (Tyler, 2000; Weigmann *et al.*, 2003). At twelve hours APF, head eversion occurs meaning the imaginal head sac is pushed into the head cavity and

the legs are fully extended (Hoshizaki, 2005; Nelliot *et al*., 2006). During the pupal stage, which occurs over four to five days, the larval tissues are destroyed or remodeled and the adult tissues are formed. The adult fly is able to lay eggs two days after eclosion (Riddiford & Truman, 1993). As a holometabolous insect, *D. melanogaster* undergoes complete metamorphosis where most larval tissues undergo apoptosis but the fat body is subject to remodeling and persists until a few days after the adult has eclosed. Since the organism cannot feed during metamorphosis, the larval fat body is necessary to provide energy for the changes that occur and to maintain the adult fly until it can find an external food source post-eclosion (Aguila *et al.*, 2007).

Metamorphosis and the larval Fat Body:

The juvenile-adult transition, from larva to adult, during metamorphosis begins at the end of the third instar larval phase and leads to the prepupal and pupal stages to generate an adult fly. During metamorphosis, the organism is unable to feed due to its immobility and must rely on the larval fat body stores to provide energy. The larval fat body cells are refractive to programmed cell death, allowing them to persist after this process removes many of the larval tissues. Instead, the fat body cells are remodeled and become individual free floating cells as seen in Figure 2. The remodeled larval fat body cells can now move throughout the organism and fuel the necessary changes and energy requirements of the fly. The majority of the larval tissues are replaced by cells of the imaginal disks and

histoblasts that proliferate, undergo organogenesis, and differentiation to form the adult structures (Aguila *et al.*, 2007). After the fate of the imaginal disks (derived from the epithelial tissue) is determined and eversion of the legs and wings occurs, the imaginal disks develop into the adult fat body (Worley *et al.*, 2012).

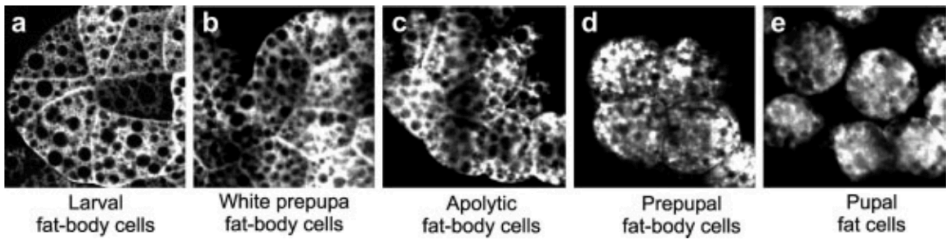

Figure 2: The changes in the shape of the larval fat body cell during different periods of development starting before metamorphosis and continuing until after fat body remodeling is completed. Larval fat-body cell cluster appearance in the a) third instar larva, b) white prepupa, c) at apolysis, d) prepupa and e) early pupa. (Nelliot *et al*., 2006).

Larval Fat Body Development:

The larval fat body is important for the maintenance of homeostasis and energy provision through the different stages of the organism including the feeding and non-feeding stages. Multiple hormones are known to affect the role of the fat body in metamorphosis but the exact mechanism and interactions are unknown. The larval fat body is located between the body wall and the midgut and is submerged in the hemolymph. In the larval stage, the fat body is composed of cells that are white and translucent in color but are flat and polygonal in shape. These cells are tightly associated in a single-cell layered sheet (Nelliot *et al.*,

2006). The larval fat body and the adult fat body are separate organs that arise from different progenitor cells at different times in the organism (Nelliot *et al.*, 2006). The larval fat body is developed from the embryonic mesodermal cell cluster (Zhang & Xi, 2014). The embryonic fat body tissue is derived from cells found at stage 10/11 (Hoshizaki, 2005). At stage 11 through 14, the progenitor cells develop from 9 clusters of cells in the inner mesodermal layer that spans parasegments 4 to 12. These clusters are located in the lateral, ventral and dorsal mesoderm and produce the fat cells of the larval fat body (Zhang & Xi, 2014). These cells form a single layer of tissue that is one cell thick and that contains the lateral fat body, the dorsal fat-cell projection and the ventral collar by stage 15/16 in embryogenesis as seen in Figure 3 (Zhang & Xi, 2014).

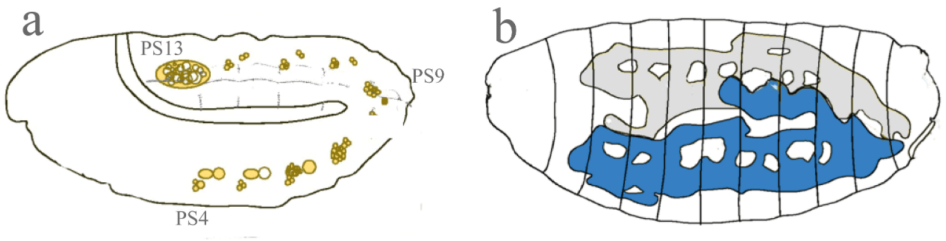

Figure 3: Scheme of the location of the precursor larval fat body cell domains in the developing embryo of *Drosophila melanogaster*. A) Represents a stage 12/13 embryo where the progenitor fat cells originate from the nine bilateral cell clusters represented by the yellow circles. B) A stage 15/16 embryo where the mature larval fat body cells form a single cell layer of fat body tissue. This monolayer expands from the abdomen to form the lateral fat body, the ventral collar and the dorsal fat-cell projection (Zhang & Xi, 2014).

The lateral fat body forms a wide ribbon on each side of the organism located in between the body wall muscle and the gut (Hoshizaki, 2005). The larval fat body is located mainly in the abdomen but there are projections in the thorax and head (Zhang & Xi, 2014). The fat body cells form two projections that extend from the posterior region of the lateral fat body and are beside the dorsal heart vessel on the dorsal side of the organism (Hoshizaki, 2005). When embryogenesis is complete there are approximately 2, 200 fat body cells which only increase in volume through the larval feeding stages to store energy. These cells persist until about 2 days after the adult fly has eclosed when they undergo programmed cell death and are replaced by the adult fat body (Zhang & Xi, 2014). The adult fat body is derived from the imaginal disks from of the ectoderm and begin to form during pupation (Nelliot *et al.*, 2006).

To aid in the process of segmentation, there are the pair-rule genes *even-skipped* (*eve*) and *sloppy paired* (*slp*). Both are expressed at stage 11 in embryo development and result in an alternating 14-stipe pattern. This patterning allows the subdivision of the parasegments (PS) into an *eve* and a *slp* functional domain. The eve protein domain corresponds to the anterior region and the slp protein domain corresponds to the posterior one. These two control the development of the fat body cells (Riechmann *et al.*, 1998). The primary fat-cell clusters in PS 4-9 are in the eve protein domain and are contained in this region with the expression of *engrailed (en)* and *hedghog (hh)* genes. After this first wave of determination,

directly behind the primary fat-cell clusters in PS 2-12, the secondary fat-cell clusters are also determined in the eve protein domain but only in the wingless protein (Wg) subdomain. In this region, *en* and *hh* are not expressed but may be present where *Slp* is expressed (Riechmann *et al.*, 1998). The secondary ventral fat-cell clusters are controlled by wg in the Slp protein domain. *slp* negatively regulates *eve* and encodes a forkhead domain transcription factor (Hacker *et al.*, 1992). The dorsal fat-cell cluster in the dorsal mesoderm, is contained in PS 13 and the eve protein domain of PS 14 (Riechmann *et al.*, 1998). srp protein is involved in the specification of the fat-cells and is a target of Ultrabithorax (Ubx). Ubx is a homeotic transcription factor that results in the repression of *arp* expression in the secondary ventral fat-cell clusters in PS 6-12 and the construction of the fat-cell bridge in PS 6. Ubx negatively controls the formation of the ventral commissure and the dorsal projections meaning that *srp* is a direct target of this transcription factor (Hoshizaki, 2005).

***Serpent / A-Box binding factor*:**

In addition to the cells that allow the production of the lateral fat body, there are two additional cell groups that give rise to the mature fat body. These two lateral and ventral secondary cell clusters were determined based on their production of *A-Box binding factor* gene (*Abf*) which is also known as *serpent (srp)*. This protein belongs to the GATA transcription factor family that allows positive regulation elements in the larval promoters of *Adh* genes that allow

transcription to occur. The expression of *Adh* marks the initiation of terminal fat-cell differentiation. *Adh* is necessary for fat-cell, hematocyte and gut formation as well as germ band retraction (Hoshizaki, 2005). The primary fat-cell cluster, composed of the lateral and ventral secondary fat-cells, is located in parasegment 4-9, the lateral and ventral secondary fat cells are located in parasements 4-12, and the dorsal fat-cell cluster is in parasegments 13 and 14. There are a total of nine bilateral fat-cell clusters with six of these located in the primary fat-cell cluster. The primary fat cells express *arp* at stage 11 and after this the secondary lateral and ventral fat-cell clusters appear and likely contract to the lateral larval fat body. PS 3-5 contains the ventral secondary cell clusters that later form two fat-cell bridges: the anterior and posterior bridges. From the posterior bridge the bilateral horns of the fat cells extend to cross the anterior bridge. The rest of the secondary fat cells in PS 6-12 form the ventral edge of the lateral fat body. The dorsal fat cells in PS 13 and PS 14 produce the bilateral projections of the fat cells and are part of the lateral fat body (Hoshizaki, 2005).

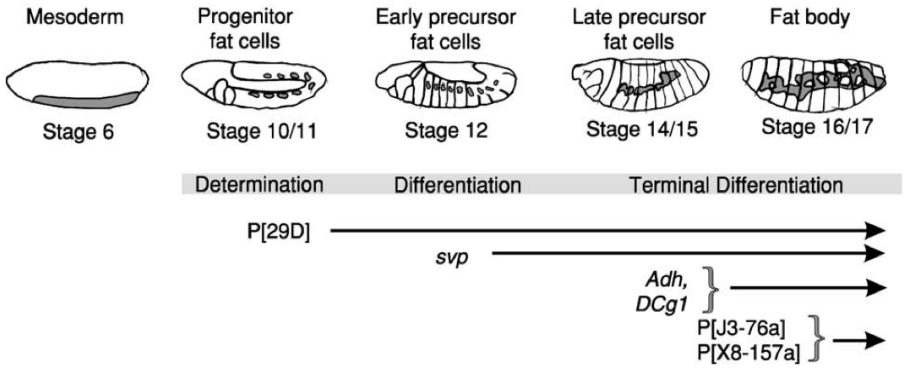

Figure 4: Lineage of the larval fat-body cells of the lateral fat body in the different stages of fat-cell development. The mesoderm first develops from the ventral region on the developing organism at stage 6 in embryogenesis. These mesodermal cells then form the nine bilateral clusters that can be observed at stage 10-11. The nine clusters then undergo expansion and the cells of the posterior region extend to form the dorsal fat body in stage 12 embryos. Terminal fat-cell differentiation in stage 15 leads to the development of the late progenitor cells thanks to the expression of *Adh* and *DCg1*. The fat body is fully formed by stage 16/17 when the enhancer-trap lines are active (Hoshizaki, 2005).

Abdominal-A and Abdominal-B:

Abdominal-A (abd-A) and Abdominal-B (abd-B) directly affect the transcription of *srp*. *abd-A* is expressed only in PS 10-12 to prevents primary fat-cell cluster formation in this area. The role of abd-A is to control the spatial organization of the primary fat body cells. abd-B similarly prevents the formation of primary fat-cell clusters when expressed in parasegment 13. However, abd-B is sufficient and necessary for fat-cell development in the dorsal mesoderm but prevents the development of fat-cells in the lateral and ventral mesoderm. abd-B also aids the formation of the somatic gonadal precursors. The concentration of

this protein controls the development or repression of the fat cells by the dorsal ventral axis of the mesoderm (Hoshizaki, 2005).

Tinman:

tinman (tin) is a NK homeodomain protein-encoding gene and is expressed at three time periods in embryonic development. During the first phase of expression, *tin* is expressed in all mesodermal tissue and induces the formation of the fat body. In the second phase, this gene determines the dorsal mesoderm. In the last phase, the expression of this gene only occurs in the heart precursor cells. Therefore, *tinman* allows for the specification of the larval fat cells (Hoshizaki, 2005).

In coordination with insulin signaling, the change in the larval fat body's role from energy storage to energy release is also indicated through important structural changes as seen in Figure 3 (Nelliot *et al.*, 2006). The appearance of the larval fat body does not change as the organism changes into a prepupa, but tissue does fill the space between the body wall and the gut. This is how the fat body appears at zero hours APF. During the next six hours, the retraction phase occurs meaning the fat body withdraws from the anterior region and the individual cells become rounder but remain tightly associated. These changes as well as apolysis (where the larval epidermis separates from the brown puparium) are complete by six hours APF (Nelliot *et al.*, 2006).

The next phase, the disaggregation phase, is complete by fourteen hours APF. During this stage, the cells of the fat body start to dissociate and become free floating cells. This process occurs in an anterior to posterior manner where the cells are pushed into the head capsule by abdominal muscular contractions inducing head eversion at 12 hours APF. Once the head is filled with fat cells, the remaining fat body cells detach and disperse throughout the open interior area of the pupa. Macrophages are then involved in the removal of the extracellular matrix that once connected the fat body cells. If proper remodeling cannot be completed, then pharate adult lethality will occur where the newly formed adult fly will be unable to eclose (exit) from its pupal case (Nelliot *et al.*, 2006).

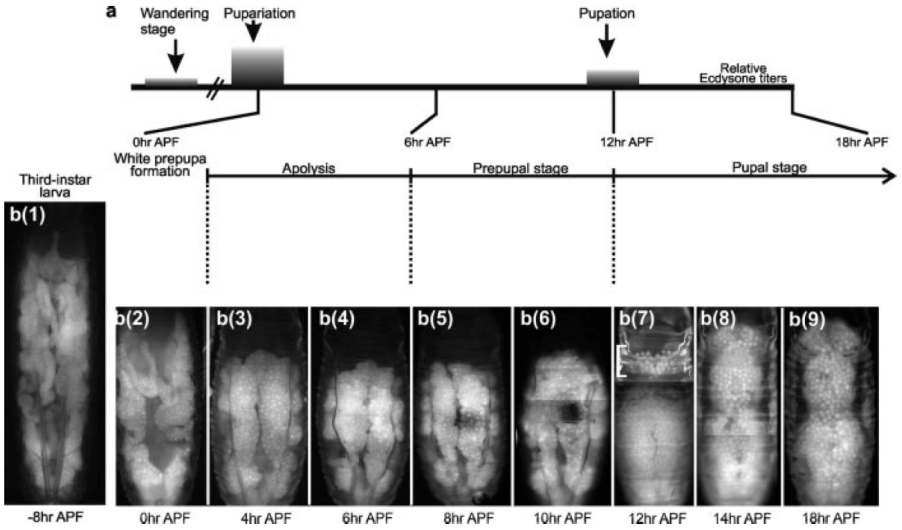

Figure 5: Fat body remodeling during metamorphosis in *Drosophila melanogaster*. Part a describes the relative ecdysone tiger during this phase of development. Part b illustrates the different remodeling stages. Starting at 0 hours APF, retraction is complete and the fat cells start to appear round by 6 hours APF. By 12 hours APF, head eversion is complete and the fat cells dissociate into free floating cells (Nelliot *et al.*, 2006).

After the fly ecloses, the fat body cells persist for another three days indicating that the fat body must gain enough energy to fuel the changes in metamorphosis and survive through early adulthood. However, these free floating cells are soon replaced by the adult fat body which once again forms a sheet of fat cells (Aguila *et al.*, 2007).

Hormones that affect fat body development:

Hormones control fat body development in a spatial and temporal manner. The two main hormones that affect the fat body are 20-hydroxyecdysone (20-E) and insulin. Both hormones use downstream signaling to aid in the transition and development from larva to adult fly.

20-hydroxyecdysone (20E):

20-hydroxyecdysone (20E) is a steroid hormone that coordinates the juvenile-adult transition in *Drosophila melanogaster* as well as in other insects. This transition occurs during metamorphosis in *D. melanogaster* in response to pulses of 20E which interacts with multiple nuclear receptors (Rewitz *et al.*, 2010). In *D. melanogaster* there are two pulses of 20E at the end of the third larval instar and at the end of the prepupal period. 20E is derived from cholesterol in the prothoracic glands (PG) and is converted into its active form only in the peripheral tissues (Herboso *et al.*, 2015). 20E functions as a ligand-regulated

transcription factor comparable to other members of the nuclear receptor superfamily. Its receptor is composed of a heterodimer of two proteins: EcR and Ultraspiracle (USP). 20E can induce the expression of stage-specific gene cascades that control the timing of the progression of development. The response to 20E signaling is tissue specific and results in cascades of gene expression that control developmental changes at specific developmental times (Riddiford & Truman, 1993). During the wandering stage, after critical weight has been attained, there is a low concentration of 20E that then spikes to initiate metamorphosis. This spike induces the start of the prepupal stage and simultaneously reduces growth through the larval fat body (Herboso *et al*., 2015, King-Jones *et al.*, 2005). 10 – 12 hours later, the prepupal 20E pulse induces the abdominal muscles to contact allowing the head cavity to be formed (head eversion) and marking the start of the prepupal-pupal transition. During the late larval 20E pulse there is activation of the so-called early genes: *E74*, *E75* and the *Broad Complex*. These three are directly activated by 20E and all code for families of transcription factors and directly affect late gene transcription (King-Jones *et al.*, 2005).

The presence of 20E signals for the destruction of larval tissues as demonstrated by the appearance of autolysosomes in response to the rise in ecdysone concentration. If 20E signaling is disrupted, the fat body does not dissociate but forms aggregates of non-dissociated cells indicating that it is

necessary for proper fat body remodeling. 20E is therefore sufficient to induce programmed cell death, puparium formation and fat body remodeling.

20E regulates transcription of the genes encoding EcR and Ultraspiacle, and it also affects the transcription of about eight other canonical nuclear receptors. However, these receptors have no known hormonal ligand and are thus called orphan nuclear receptors. DHR3 is one of these orphan receptors that, along with E75B, is used to induce expression of βFTZ-F1; a mid-prepupal competence factor (King-Jones *et al.*, 2005). βFTZ-F1 is necessary and sufficient to induce the response expected from 20E signaling at the prepupal pulse (King-Jones *et al.*, 2005).

βFTZ-F1:

βFTZ-F1 is a competence factor for a cellular genetic response to the prepupal 20E pulse, around 10-12 hours APF, that induces adult head eversion and the prepupal-pupal transition (Ruaud *et al*., 2010). This response includes the expression of the genes encoding E74A and E75A and E93. *βFTZ-F1* encodes transcriptional factors that code for members of the nuclear receptor superfamily. The *ftz-f1* gene encodes two protein isoforms: αFTZ-F1 and βFTZ-F1. The former functions as a cofactor for the *fushi tarazu (ftz)* segmentation gene. *βftz-f1* is only expressed in late embryonic, larval and pupal stages and when mutated results in embryonic lethality. βFTZ-F1 is necessary for maturation of the cuticular denticles. DHR3 is also expressed at the same time and has an overlapping

transcriptional response to βFTZ-F1 that indicates a functional bifurcation in response to 20E signaling (Ruaud *et al.*, 2010).

βftz-f1 expression depends on the decrease in titter of 20E after puparium formation. *βftz-f1* expression is controlled by DHR3, DHR4 and dBlimp-1. dBlimp-1 is produced in response to the late larval 20E pulse and then this protein directly binds the *βftz-f1* promoter then is degraded. The quick expression of dBlimp-1 allows the tight regulation of βFTZ-F1 produced in response to the late larval 20E pulse. βFTZ-F1 induces the transcription of the genes necessary to promote head eversion, salivary gland cell death, and leg and wing extension (Bond *et al.*, 2011).

βFTZ-F1 is also sufficient to cause fat body remodeling during metamorphosis. This is because matrix metalloproteinase 2 (MMP2) is a protease that cleaves the ECM and is a downstream target of βFTZ-F1. There are two MMPs but both are sufficient and necessary for fat body remodeling (Bond *et al.*, 2011).

E93:

Combined with βFTZ-F1, BR-C and E74A, E93 is necessary for the destruction of the salivary glands in response to 20E signaling. While the βFTZ-F1 protein is sufficient to trigger the late cell death genes that are responsible for salivary gland cell death, E93 is necessary for βFTZ-F1 regulation in this pathway and induction of the late cell death genes: *rpr, dronc* and *crq*. βFTZ-F1 controls

the timing of the 20E cellular responses while E93 is vital to the 20E cell death response (Lee *et al.*, 2002). E93 is also expressed in the fat body at 12 hours APF when the fat body undergoes remodeling. E93 does not trigger programmed cell death in the larval fat body but it may influence its remodeling (Lam, 2012).

MMPs:

Matrix metalloproteinases (MMPs), are proenzymes composed of a catalytic domain and an auto inhibitory pro-domain. Each contains a signal that indicates if they are to be secreted or attached to the plasma membrane of a cell. Membrane-type MMPs are attached to the plasma membrane through a glycosylphosphatidyllinositol (GPI) -anchored domain or a transmembrane domain (Jia *et al.*, 2014). MMPs are responsible for the cleavage of the components of the ECM including collagen and laminin (Bond *et al.*, 2011). There are many types of MMPs depending on the organism but there are also four types of tissue inhibitors of metalloproteinases (TIMPs) that prevent the action of MMPs. There are only two MMPs in *Drosophila melanogaster* (MMP1 and MMP2) and one TIMP. This is a much simpler system compared to the 23 MMPs in humans. *Drosophila* MMP1 is a secreted protein while MMP2 is GPI anchored (Jia *et al*., 2014). Both MMPs share a conserved domain structure and a conical structure that likely allows them to degrade the basement membrane (BM) components and are involved in tumor invasion (Bond *et al.*, 2011; Jia *et al.*, 2014). MMP1 and MMP2 expressed together are necessary and sufficient to cause

the cells of the fat body to dissociate. MMP1 and MMP2 each have distinct roles but work cooperatively to allow cellular separation. MMP1 primarily digests the cell-cell junctions but also assists with the cleavage of the basement membrane (Jia *et al.*, 2014). MMP1 expression is simultaneous with the 20E mediated salivary gland cell death and may participate in this pathway as well (Bond *et al.*, 2011). MMP2 has a different role; it primarily digests the basement membrane and assists with cell-cell junctions (Jia *et al.*, 2014).

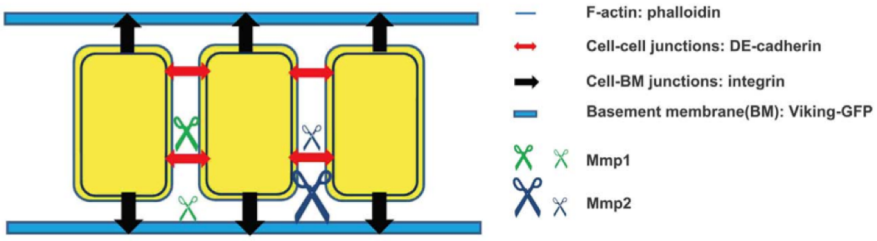

Figure 6: MMP1 and MMP2 work cooperatively to allow the separation of the cells of the larval fat body. Mmp1 and Mmp2 have their separate roles but both work to separate the cells. Mmp1 primarily cleaves the cell-cell junctions whereas Mmp2 is the major contributor to the digestion of the basement membrane (Jia *et al.*, 2014).

Insulin/PI3K Pathway and ecdysone:

The Tor and PI3K pathways negatively regulate autophagy, programmed cell death and tissue remodeling. Ecdysone receptor signaling has the opposite effect and induces autophagy. For autophagy or remodeling to occur during metamorphosis, ecdysone signaling is necessary to down regulate PI3K signaling (Rusten *et al.*, 2004).

Class 1 phosphoinositide 3-kinase (PI3K) is a downstream component of tyrosine kinase receptors in the insulin signaling pathway. PI3K allows the formation of phosphatidylinositol-3,4,5-trisphosphate (PIP_3) and is a repressor of autophagy and tissue remodeling. The level of expression of PIP_3 is regulated by being dephosphorylated by the phosphatase and tension homolog deleted from chromosome 10 (PTEN). PTEN can therefore prevent autophagy (Rusten *et al.*, 2004).

Target of rapamycin (Tor) is a kinase that is necessary in regulating the starvation responses including that experienced by *D. melanogaster* during metamorphosis. Rapamycin induces autophagy by targeting the inactivation of Tor. This means that Tor is a negative regulator of autophagy and is also affected, similarly to PI3K, by the presence of 20E (Rusten *et al.*, 2004). For the destruction of the larval tissues and larval fat body remodeling to occur, 20E signaling must down regulate the Tor and PI3K pathways.

TGFβ:

The larval fat body remodels in response to 20E during metamorphosis, while other tissues respond by undergoing programmed cell death. For this reason, it is likely that 20E is connected to other cell pathways that control the remodeling of the fat body. Transforming growth factor β (TGFβ) is a secretory polypeptide family whose signaling disruption causes premature dissociation of the larval fat body cells. TGFβ interacts with other receptors and Smads that

control the transcription of genes. It is likely that these downstream genes affect adhesion molecules, proteases or other proteins involved in the degradation of the connective proteins between the fat body cells. The four TGFβ relayed factors are decapentaplegic (Dpp), Glass-Bottom-Boat (GBB), Screw and Activin. These factors function as dimers and signal through transmembrane protein serine/threonine kinases that are either type I or type II receptors. TGFβ unites the two parts of the dimer together to phosphorylate the type I receptor to activate the type I receptor kinase. Smad proteins Mad (*mothers-against-decapentaplegic*) and Medea are then phosphorylated and can then function as transcription factors (Hoshizaki, 2005). Smads are a family composed of receptors (R-Smads, Mad and dSmad2), a shared Smad (Co-Smad, medea) and an inhibitory Smad (I-Smad and Daughter against Decapentaplegic (Dad)) (Raftery and Sutherland, 1999). Mad/Medea is responsible for transducing Dpp signaling. GBB signaling affects fat body morphology but is independent of Dpp signaling. GBB signaling controls the morphology of the fat body by acting through Sax, Mad and Medea (Hoshizaki, 2005).

All TGFβ ligands signal through Punt, a type II receptor, but use unique type I receptors. Saxophone (Sax) is the type I receptor that mediates GBB signaling and if mutated leads to embryonic lethality. However, the sax4 allele is temperature sensitive where larvae cultured at 18˚C fail to pupate but can reach the late-third instar larval stage of development (Hoshizaki, 2005). TGFβ therefore maintains the intact structure of the fat body through the help of Smad

proteins. 20E is able to influence the presence of TGFβ so that the fat body can remodel during metamorphosis (Hoshizaki, 2005).

There are multiple genes and proteins involved in metamorphosis and larval fat body remodeling that are all connected in a series of interactions. A summary of the major genes and proteins involved in fat body remodeling is summarized below in Figure 7.

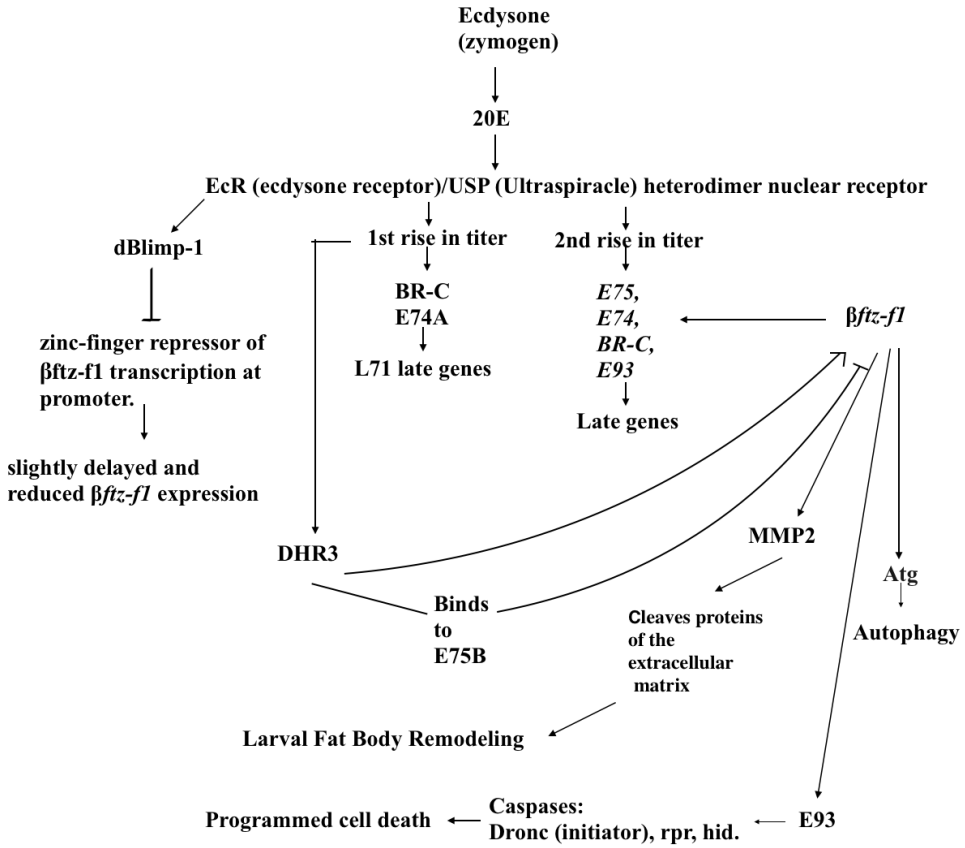

Figure 7: Summary of the major proteins and genes involved in metamorphosis and fat body remodeling. Arrows indicate that the gene/protein of origin induces the expression or action of the gene/protein the arrow points towards. The blunt ended lines indicate that the gene/protein of origin inhibits the expression or action of the gene/protein the line leads towards.

Pharate Adult Lethality:

Pharate adult lethality occurs when the organism develops into an adult fly that is unable to eclose from its pupal case at the pharate stage and is associated with the inability of the fat body to properly remodel. This explains why larval fat body remodeling is a necessary event to complete metamorphosis. Remodeling allows the redistribution of the newly separated fat cells throughout the body of *Drosophila melanogaster*. The cause of lethality has not been determined (Nelliot *et al.*, 2006). Given the complex interplay of hormones and other signaling molecules, it is possible that there are multiple causes for this lethal phenotype. This genetic screen was conducted as an attempt to determine the genes involved in pharate adult lethality.

Principles of a Broad Genetic Screen in fat body remodeling:

A genetic screen is an attempt to identify certain genes that cause an abnormal phenotype by implementing a mutagenesis. After a mutagenesis was performed, the mutated fly lines in this genetic screen were first selected for pharate adult lethality and then for abnormalities in the fat body remodeling. This type of screen allows for an absence of bias in the determination of novel genes involved in larval fat body remodeling because no specific genes could be targeted to contribute to a specific phenotype (Walchessen, 2016).

Due to the numerous biochemical signaling pathways involved in fat body remodeling, there is a possibility of determining new genes involved in the larval fat body remodeling process in response to the 20E titer increase (Nelliot *et al.*, 2006). These novel genes could provide key insights into the homologous remodeling process used in wound health and metastasis in higher order organisms.

Aurora-A:

One of the pharate adult lines (*aur-A*^{14641}) that experiences partial fat body remodeling, has already been mapped to gene called *Aurora-A* (*aur-A*) (Gausz *et al.*, 1981). The gene codes for a serine/threonine protein kinase that is highly conserved (Moon & Matsuzaki, 2013). The regulation of this kinase in time and space is necessary for the coordination of important cellular events (Sabino *et al.*, 2010). There is a homologous gene in mammals that belongs to a family of Aurora kinases that are important regulators of multiple cellular events. Mutations in *aurora-A* result in developmental defects and can affect multiple phenotypic traits such as abnormal centrosome spindle behavior and positioning, problems in chromosome segregation, an absence of astral microtubules, cortical targeting of fate determinants and self-renewal of neural stem cells (Sabino *et al.*, 2010). Aurora-A allows for the asymmetrical localization of aPKC in the apical cortex where aPKC can then negatively regulate Numb that in turn negatively regulates Notch signaling to allow for neuroblast self-renewal as seen in figure 7 (Wang *et*

al., 2006). Notch is a transmembrane receptor that is cleaved to affect transcriptional regulation. Aurora A uses Mud to regulate the spindle orientation to achieve cell differentiation through asymmetrical division. This is how Aur-A acts as a tumor suppressor.

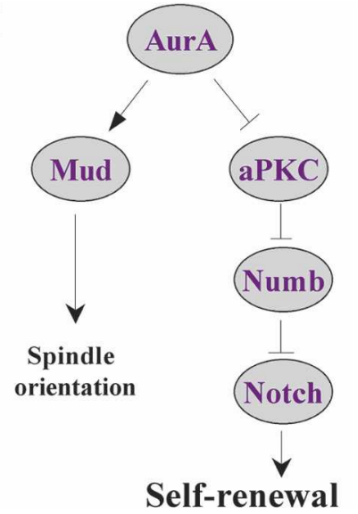

Figure 8: Model of how Aur-A interacts with Notch and aPKC to control neuroblast self-renewal. Aur-A interacts with Mud to allow asymmetrical localization therefore influencing spindle orientation. The direct interaction of Aur-A with aPKC is unknown (Wang *et al.*, 2006).

Aur-A is also regulated by different cofactors and activators. One of these is TPX2 that can bind Aur-A to allow auto-phosphorylation and targets it to the mitotic spindle. Aur-A then activates Bora that when mutated causes problems with the asymmetric division of the sensory organ precursors (SOPs). Ajuba contains an LIM domain that localizes it to the sites of cell-cell adhesions in epithelial cells and activates Aur-A and localizes to the centrosome. Ajuba mutants die at the larval-pupal transition. This means that Ajuba is responsible for

maintaining active Aur-A at the centrosome during mitosis *(*Sabino *et al.*, 2010). The role of Aur-A in neuroblasts is well studied and described to have an active role in the cytoskeletal arrangement during mitosis. Aur-A is a known regulator of microtubule dynamics but it is also participates in the processes that involve actin cytoskeleton. If Aur-A is over expressed, cytokinesis fails in the cultured cells (Moon & Matsuzaki, 2013). This means that Aur-A has a role in microtubule and actin organization.

Three lines from the original mutagenesis have been mapped to the *aurora A* gene: $aur\text{-}A^{14641}$, $aur\text{-}A^{8839}$ and $aur\text{-}A^{17961}$ (Wang *et al.,* 2006). All of these lines experience a massive increase in levels of neuroblast cells by more than a hundred fold (Lee *et al.*, 2006). $aur\text{-}A^{14641}$ has a single base pair change from valine, a nonpolar and hydrophobic amino acid, to glutamic acid, a polar and charged amino acid, at position 302 located in the kinase activation loop. The differences in properties of these amino acids can have many possible detrimental effects. This line experiences pharate adult lethality and partial fat body remodeling (Lee *et al.*, 2006).

$aur\text{-}A^{17961}$ also has a single nucleotide change that results in a destabilization in the alpha helical packaging. The mutation is a change from aspartic acid, a polar and charged amino acid, to asparagine that is polar but uncharged and a more bulky amino acid at position 334 (Lee *et al.*, 2006). This line does not survive to the pupal stage and dies as a third instar larva but many do not survive to this stage.

The final line, *aur-A*^{8839}, experiences the most severe mutation from lysine to a stop codon at position 377 that truncates the protein (Lee *et al.*, 2006). This line is pharate adult lethal. A summary of these mutations is found in Figure 8.

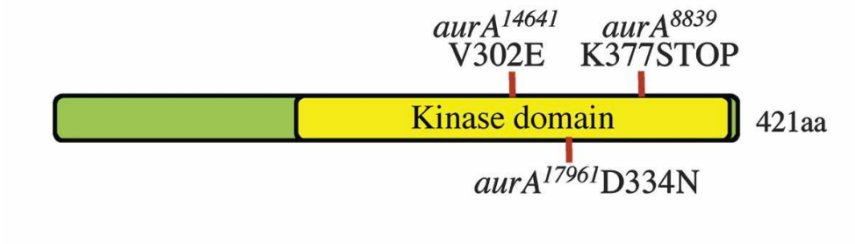

Figure 9: Scheme of *aur-A* mutations in lines *aur-A*^{14641}, *aur-A*^{8839} *and aur-A*^{17961} and the location of *aur-A*. (Wang *et al.*, 2006).

Hypotheses and aim of study

The aim of this study is to determine if there are abnormalities in larval fat body remodeling in the mutated fly lines created from the EMS mutagenesis performed by Wang *et al.*. Due to the inability of the mutated pharate adults to eclose from their pupal case, it can be inferred that abnormalities in larval fat body remodeling are causing insufficient energy supply to allow flies to exit their pupal case. I hypothesize that dissections of the mutant lines during metamorphosis will show abnormalities in larval fat body remodeling and how severe they are. The number of genes involved in the fly lines with severe remodeling deficits were determined by crossing the mutated lines to each other and dissecting the progeny's larval fat body during metamorphosis. I also hypothesize that the mutated gene causing the most severe abnormalities in

remodeling can be mapped to its chromosomal location to determine how this gene affects remodeling. Three lines have already been mapped to a gene, *aur-A*. However, the function of this gene in larval fat body remodeling is unknown but I hypothesize that it affects the cytoskeletal arrangement. To help elucidate the function of this gene in remodeling, the actin filaments were visualized at 0 and 10 hours APF in the mutants and wild-type flies to determine if there are any differences caused by this mutation.

MATERIALS AND METHODS

Drosophila stock Husbandry:

All mutated fly lines were donated by Dr. Arash Bashirullah from the University of Wisconsin after their generation by Wang *et al.* (Wang *et al.,* 2008). The mutated lines and w^{1118}, acting as a control, were kept on standard agar food and kept at 25˚C. Vials were transferred every other week while bottles were transferred weekly. Virgin females and males to be used in the complementation tests were kept at 18˚C until they were needed.

Generation of the mutated lines:

The mutated fly lines were obtained from Wang *et al.* and were generated from w^{1118} lines that were isogenized for the third chromosome. Figure 9 shows the crossing protocol that was performed. w^{1118} flies were aged for 3-4 days then removed from any source of food for 8-12 hours and then fed 10nM EMS in 5% sucrose for a following 12- 24 hour period. After EMS was ingested, the males recovered for hours on normal food. During this time, virgin females that contained a reporter transgene, phenotypic markers and a balancer chromosome were collected. 25 recovering males were then crossed to 50 of these female virgin flies per bottle. The F_0 bottle was transferred every day for the next four days. The F_1 males were then isolated and crossed to 3-5 females with multiple markers. Each F_2 population had a unique mutation on the third chromosome and

were given a specific number. The F_2 population was then scored for lethality. Absence of the dominant marker *Tubby* located on the balancer chromosome *TM6B, Hu, Tb* was used to identify homozygous mutants. The homozygotes were then scored for lethality by identifying the number of empty pupal cases. If the line contained 75% of homozygous mutants that died during metamorphosis, they were selected for this screen (Wang *et al.,* 2008). From the 8, 636 lethals there were only around 50 pharate adult lethal lines.

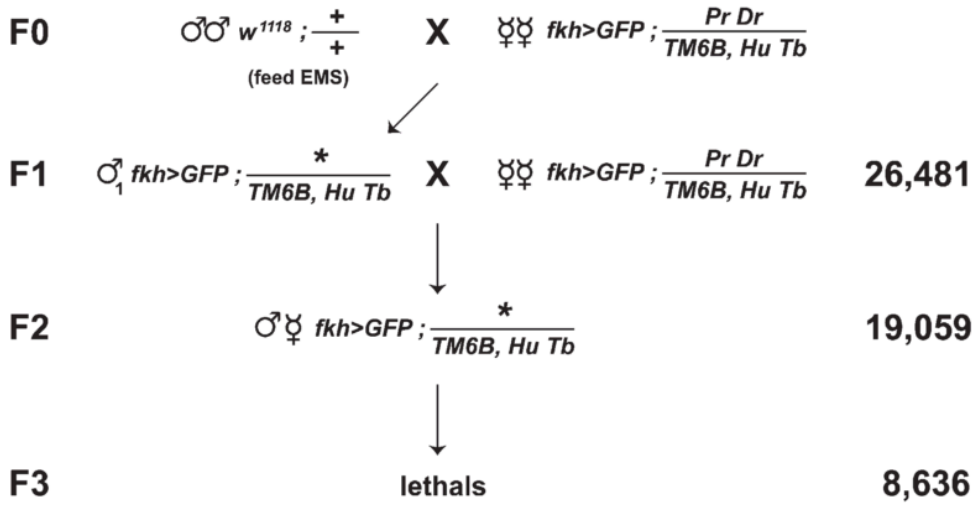

Figure 10: Genetic screen for pharate adult lethal *Drosophila melanogaster* lines (Wang *et al.*, 2008). w^{1118} males were given 10mM EMS and crosses to females containing a GFP marker, on the X chromosome, that is only expressed in the larval salivary glands (fkh.GFP ¼ w^{1118}, {fkh-GAL4}, {UAS-GFP}) as well as dominant markers *Pr Dr* and a Tubby-marked balancer on the third chromosome (*TM6B, HuTb*). In the F_1 progeny, the males were then back crossed to identical females used in the F_0 generation. Each of the F_2 progeny carried a unique mutation on the third chromosome. Stabile lines with unique mutations were established in the F3 generation and the lethal lines were determined. From these 8,636 lethal lines, around 50 pharate adult lethal lines were found (Wang *et al.*, 2008).

Dissections

At 0 hours APF, pupae that did not display the tubby dominant marker were selected to be dissected 14 hours later. These pupae were kept in a petri dish lined with a damp filter paper. The petri dishes were then stored in a plastic container lined with damp paper towels and left to age the flies to 14 hours APF at 25 ºC. At this later time point, the fat body of these flies was dissected in 1X phosphate buffered saline (PBS), visualized using a Nikon SMZ1500 stereomicroscope and imaged using a SPOT Insight QE camera linked to SPOT Imaging Solutions 5.0 software. These photographs were then saved to the hard drive and uploaded to Google drive. Photos were adjusted for levels using Photoshop CS5 and a scale bar was added with ImageJ. Once 8-10 flies were imaged for each cross, the phenotype of the fat body remodeling was then determined to be similar to the wild-type remodeling, partial remodeling or no remodeling.

Complementation crosses

For each cross, 8-10 virgin female flies were placed in a vial with 5-8 male flies from a different line. These vials were then stored at 25℃ for three days giving the females time to lay eggs and then the parental flies were transferred to a separate vial to obtain more progeny from this cross. The F_1 generation was used for dissections to categorize the fat body. Only the seven no remodeling lines were used to determine the number of different genes involved

in this phenotypic category.

Pharate Adult Lethality:

After the F_1 generation from the complementation tests had eclosed or died, the number of empty pupal cases was examined to determine if the resulting progeny were pharate adult lethal. No pupae were collected for dissections after the F_1 generation started eclosing.

Mapping:

All mapping stocks were donated by Dr. Arash Bashirullah from the University of Wisconsin and were originally obtained from the Bloomington *Drosophila* Stock Center (BDSC). These stocks were used by Sapiro *et al.* in their mapping experiment and I used the same method to map these mutations (Sapiro *et al.*, 2013). This mapping technique uses four pairs of dominant markers that all have known positions on the third chromosome: *Roughened (R), Dichaete (D), Glued (Gl), Stubble (Sb), Hairless (H) and Prickly (Pr).* A balancer chromosome was also used and was marked almost complete loss of humoral (*TM6B, Hu*) (Sapiro *et al.,* 2013).

In the parental generation, the male fly containing the unknown mutation was crossed to a virgin female stock containing two dominant markers. The F_1 female progeny then have the unknown mutation and the two dominant markers.

This female was then crossed back to males from the mutated line. The F_2 progeny is scored for the loss of all markers. If the unknown mutation is located inside the pair of dominant markers, then the recombination events will result in splits with different ratios. These ratios determine where the mutation is located relative to the dominant markers. If the ratios indicate that the mutation is located inside the dominant markers, meaning that there are few wild type flies, then Equation 1 can be used to determine the approximate location of the gene.

Equation 1: Recombination mapping equation (Sapiro et al., 2013)

$$\frac{(loss\ of\ left\ marker)}{(loss\ of\ left\ marker) + (loss\ of\ right\ marker)} \times (cM\ between\ markers) + (cM\ of\ left\ marker) = map\ position\ in\ cM$$

Equation 1 uses the loss of the left and right markers in a weighted average to estimate the location of the unknown mutation relative to the left marker. Every cross uses only two dominant markers, a left and right one, with each pair of dominant markers located at either end of the third chromosome. Loss of the left marker, or right marker, is identifiable by the absence of the visible phenotype it causes. Absence of both markers are the wild type flies and are counted in the loss of both markers. The centimorgans (cM) between the markers in the measurable distance between the two dominant marker genes on the chromosome. The centimorgans of the left marker is the position of this gene on the left chromosome (Sapiro et al., 2013).

Once this position is determined then a candidate gene can be identified, and the mutation can be sequenced (Sapiro *et al.*, 2013). This mapping scheme is demonstrated below in Figure 10.

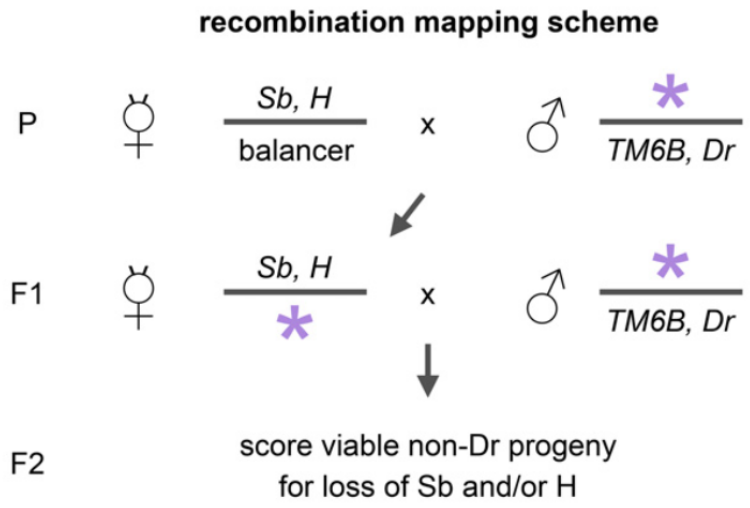

Figure 11: Mapping scheme used to determine the approximate chromosomal location of the mutations in the no remodeling lines. Using paired dominant markers *Sb* and *H* as an example, this figure illustrates how the parental lines would be crossed. The male parental (P) mutants are crossed to virgin females with the two dominant markers located on the same third chromosome. The unknown mutation is represented as a purple star. The resulting F_1 virgin female progeny that contain the unknown mutation and the dominant marker, were then back crossed to the parental male with the unknown mutation. The F_2 progeny are then scored for the loss of *H* or *Sb* (*Sb*+, *H*+ or ++ progeny) (Sapiro *et al.*, 2013).

Fluorescence imaging:

0 hour APF and 10 hours APF pupae from lines w^{1118}, $aur\text{-}A^{14641}$, $aur\text{-}A^{8839}$ had their fat body dissected on a regular slide in 1X phosphate buffered saline (PBS). Only the fat body was transferred to another slide with PBS to act as

a wash to clear any debris. The fat body was then incubated for 10 minutes in a solution of 4% paraformaldehyde in PBS to fix the cells. The fixative was removed by transferring the tissue to PBS. To allow the fluorescent dyes to enter the cells of the fat body, the cells were immersed for 5 minutes in a permeabilizer composed of 0.5% Triton X-100 in PBS. Again, the cells were washed in PBS before they were immersed in three drops of rhodamine phalloidin and Tubulin Tracker Green and kept in the dark for 45 minutes. Alternatively, for only actin staining, the cells were incubated in rhodamine phalloidin for 30 minutes. After, the cells were washed three times in PBS, they were stained in three drops of DAPI for 5 mins. Before examining under the fluorescent microscope, the cells were washed in PBS and a coverslip was placed on top of the depression slide (Cytoskeleton Inc,). The final slide was imaged with DAPI, TRITC and FITC filters with a Nikon Camera and imaged with NIS elements software. Photos were then adjusted for levels using Photoshop CS5 and a scale bar was added with ImageJ. This process was performed with 0 and 10 hour APF flies only. Once 8-10 flies per line were observed, the cytoskeletal arrangement was compared to the wild type to determine if there were any abnormalities in the mutant *aurora-A* lines.

RESULTS

Categorization:

The initial part of this genetic screen included classifying the fat body remodeling phenotype for multiple *D. melanogaster* mutant pharate adult lethal lines. There are three possible categories: wild-type, partial remodeling and no remodeling. Wild-type remodeling is visible in Figure 11 with the dissected fat body of w^{1118} which has no genetic mutations involved in fat body remodeling. If mutants only possessed larval fat body cells that are round and free floating, they were placed in the wild-type remodeling group. The results obtained from previous researchers seem to indicate that there were four lines placed in this group as seen in Table 1 (Walchessen, 2016).

The partial remodeling phenotype is defined as having some remodeled cells but with some clumps of larval fat body cells. In Figure 12, the line I(3)LL-14641: L 04 PA dissected at 14 hours APF appears to have some visible round cells but there is a presence of small clumps of cells. This mutation must produce enough functional protein to allow some of the cells to change from polygonal cells connected in a sheet to spherical cells that are free floating. For this reason, it was determined that the I(3)LL- 14641: L 04 PA line would be placed in the partial remodeling group. There were 12 other lines that were placed in this group by previous researchers as seen in Table 1 (Walchessen, 2016).

Lastly, the no remodeling phenotype is characterized by the presence of multiple or one large clump(s) of cells with very few spherical free-floating cells. This phenotype indicates that there is no, or very little, functional protein for remodeling to occur. The appearance of I(3)LL- 11075: L 04 PA is very different from the wild type phenotype and the partial remodeling phenotype seen with I(3)LL- 14641: L 04 PA. In Figure 13, the larval fat body appears to only have large clumps with some debris clearly indicating the no remodeling phenotype. Six other lines were placed in the no remodeling group by previous researchers as seen in Table 1 (Walchessen, 2016).

Table 1: Classification of mutated *D. melanogaster* lines into the abnormal groups.

Category	Mutated *D. melanogaster* lines
Wild-type remodeling	I(3)LL- 11049: L 04 PA, I(3)LL- 11224: L 04 PA, I(3)LL- 11961: L 04 PA, I(3)LL- 18835: L 04 PA.
No remodeling	I(3)LL- 11075: L 04 PA, I(3)LL- 13567: L 04 PA, I(3)LL- 15379: L 04 PA, I(3)LL- 15413: L 04 PA, I(3)LL- 17770: L 04 PA, I(3)LL- 2310: L 04 PA, I(3)LL- 7275: L 04 PA.
Partial remodeling	I(3)LL- 2536: L 04 PA, I(3)LL- 3284: L 04 PA, I(3)LL- 4994: L 04 PA, I(3)LL- 6128: L 04 PA, I(3)LL- 7749: L 04 PA, I(3)LL- 11250: L 04 PA, I(3)LL- 14641: L 04 PA, I(3)LL- 15600: L 04 PA, I(3)LL- 17019: L 04 PA, I(3)LL- 17514: L 04 PA, I(3)LL- 18867: L 04 PA, I(3)LL- 19028: L 04 PA.

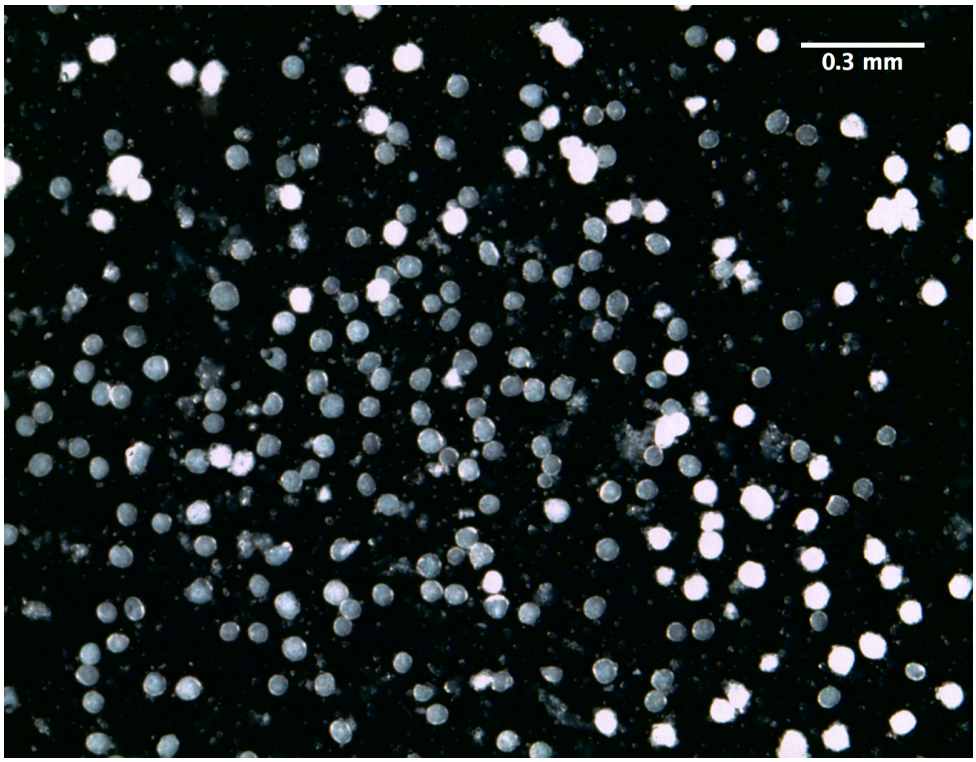

Figure 12: Wild-type fat body dissected from *w*^{1118}. *w*^{1118} 0 hour APF pupae were isolated and placed on a moist filter paper in a petri dish and incubated at 25˚C for 12 hours. The fat body was the dissected in 1x PBS and photographed at 12 hours APF.

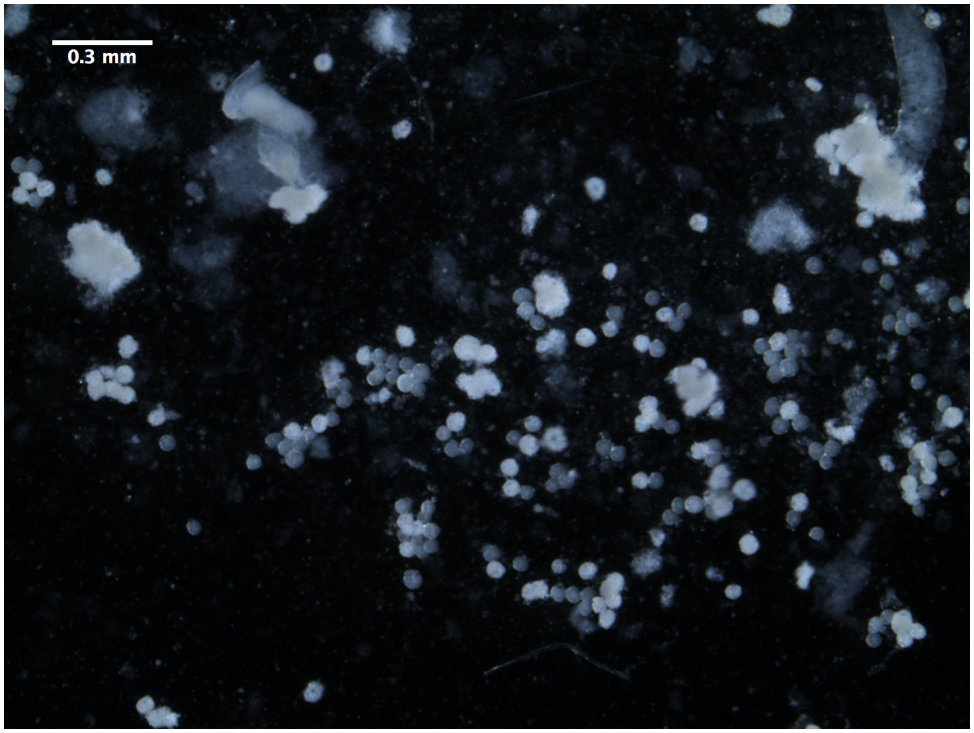

Figure 13: I(3)LL-14641: L 04 PA larval fat body dissected at 14 hours APF. 0 hour APF pupae were collected on a damp filter paper in a petri dish and incubated at 25˚C for 14 hours. The larval fat body was the dissected in 1x PBS and photographed at 14 hours APF. There are some visible round cells and small clumps of cells.

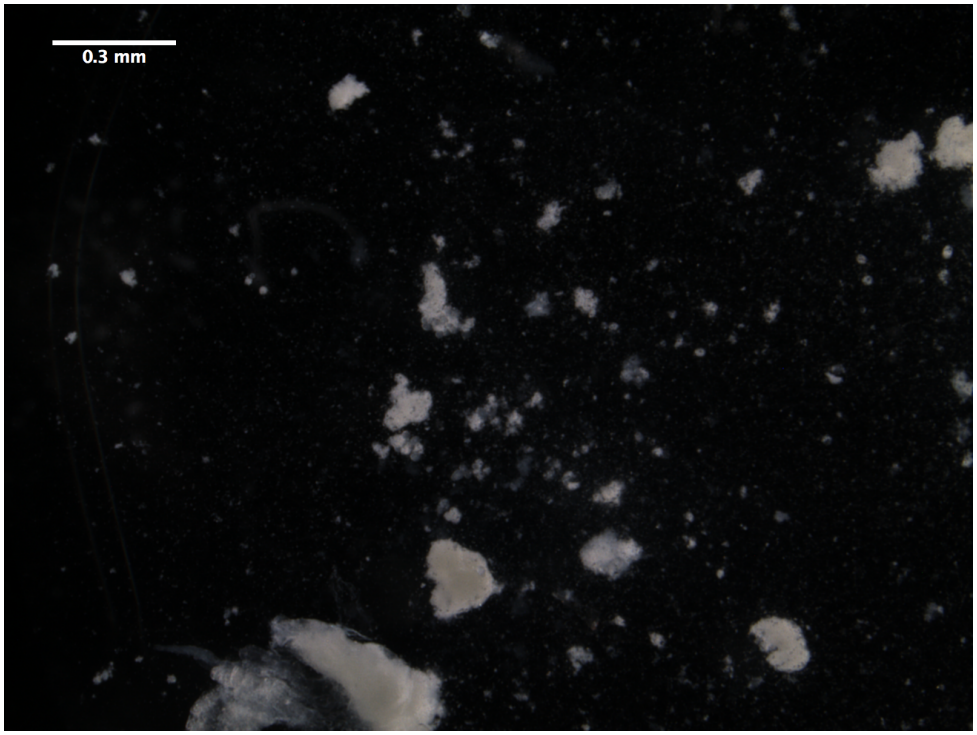

Figure 14: I(3)LL- 11075: L 04 PA larval fat body dissected at 14 hours APF. 0 hour APF pupae were collected on a moist filter paper in a petri dish and incubated at 25˚C for 14 hours. The larval fat body was the dissected in 1x PBS and photographed at 14 hours. There are large clumps of larval fat body cells and very few remodeled cells.

Images of the other no remodeling lines are included in the appendix.

Complementation tests:

It was determined that there were seven no remodeling lines. These lines were of interest since they produced the most severe abnormalities in remodeling. Crosses between each of the no remodeling lines were performed to determine if the same gene was mutated. While the progeny from the no remodelling crosses

were not pharate adult lethal, the progeny all possessed abnormalities in larval fat body remodeling as can be seen in Figures 14 and 15. This means that the pharate adult lethality phenotype complemented but the fat body remodeling phenotype did not. Interestingly, progeny of the crosses between the original mutant parental lines displayed different levels of partial remodeling. Some possessed larger or more numerous clumps while others had few clumps and more free floating round cells. For example, the cross from Figure 15 shows more extensive remodeling than that of Figure 14. Images from the other crosses that were performed are included in the appendix.

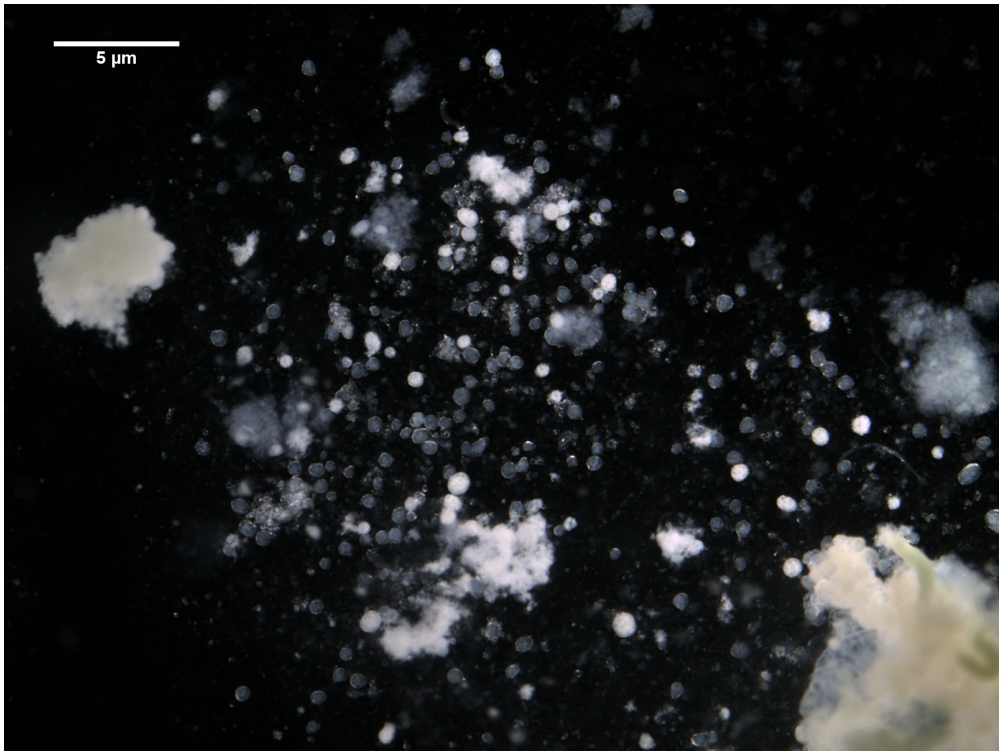

Figure 15: Larval fat body dissection of the progeny of I(3)LL-13567: L 04 PA virgin females crossed to I(3)LL-15413: L 04 PA males. The flies were dissected at 14 hours APF. This image clearly shows partial remodeling with some clumps of fat body cells which have clearly not remodeled (top left corner) and some free-floating cells (center). Pupae were collected at 0 hours APF and placed on a damp filter paper in a petri dish that was enclosed in a container with moist paper towels and left to age to 14 hours APF in a 25℃ incubator. Dissections took place in 1x PBS on a depression slide.

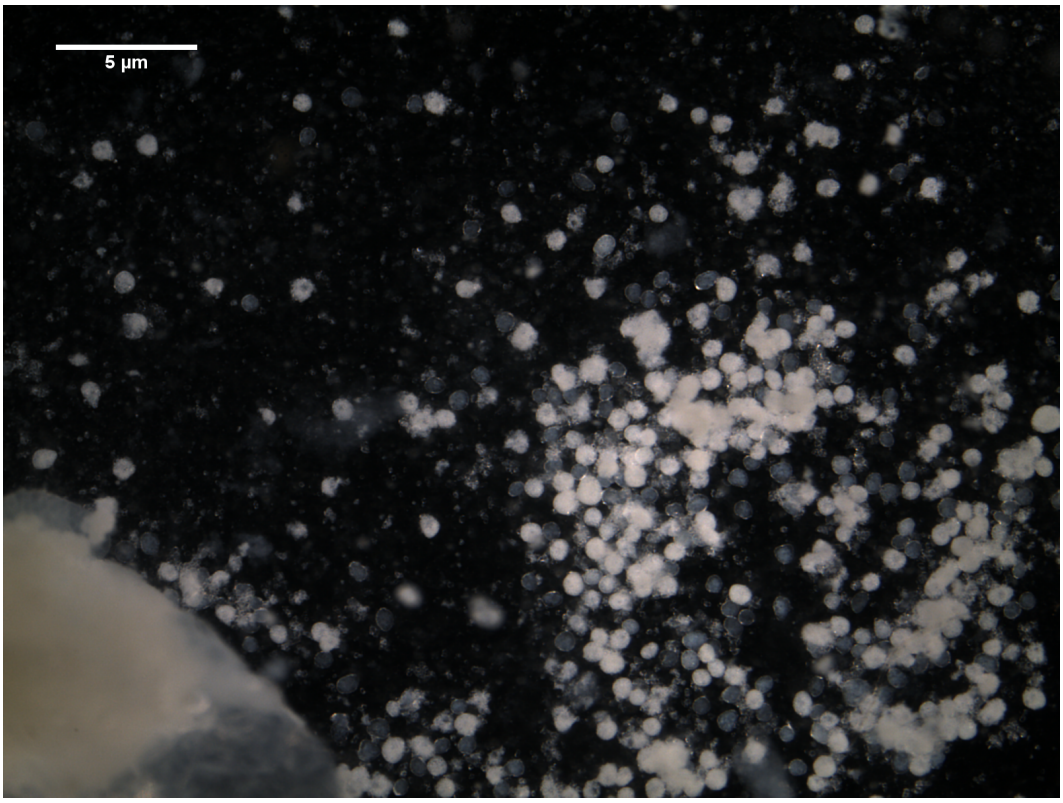

Figure 16: Dissection of the progeny of the I(3)LL-2310: L 04 PA virgin females crossed to I(3)LL-17770: L 04 PA males. The flies were dissected at 14 hours APF. This image clearly shows partial remodeling multiple cells that appear spherical and loosely connected in the center of the image but there are some individual remodeled cells as well (top left corner). The pupae were collected at 0 hours APF and placed on a moist filter paper in a petri dish that was enclosed in a container with damp paper towels and left to age to 14 hours APF in a 25℃ incubator. Dissections took place on a depression slide in 1x PBS.

Linkage Mapping:

Four of the no remodeling lines were chosen for their mutations to be mapped to their chromosomal location. These lines were: I(3)LL-11075: L 04 PA, I(3)LL-7275: L 04 PA, I(3)LL-13567: L 04 PA and I(3)LL-15413: L 04 PA.

Looking at the splits of the dominant markers *R* and *D*, and *H* and *Pr*, it was determined that I(3)LL-7275: L 04 PA is likely located between *H* and *Pr* and that I(3)LL-13567: L 04 PA is likely between *R* and *D*. The splits for I(3)LL-11075: L 04 PA were inconclusive given the small amount of progeny and their relative ratios in phenotype. As for I(3)LL-15413: L 04 PA, the preliminary data suggests that this mutation is outside of both the *H, Pr* and *R, D* pairs. The I(3)LL-15413: L 04 PA mutation is hypothesized to not be located at the ends of the third chromosome but at a more central location between 40.7cM (location of *D*) and 69.5cM (location *H*).

Using equation 1 provided by Sapiro *et al*., in the appendix, the location of I(3)LL-7275: L 04 PA was estimated to be 81.14cM. Using equation 2 in the appendix, the location of I(3)LL-13567: L 04 PA was calculated to be approximately 29.8586cM.

Fluorescence Microscopy:

One of the mutations has previously been determined to be *aura-A* for three lines: *aur-A*^{14641}*, aur-A*^{17961} and *aur-A*^{8839}. Since the *aura-A* gene appears to control cytoskeletal arrangement, the actin and microtubule filaments were fluorescently labeled and compared to wild type w^{1118} flies. The microtubule stain was unsuccessful in providing clear images so no remarks could be made on its organization in the wildtype or mutant lines.

However, the actin stain gave clear images that allowed comparisons between the wild-type and mutant lines. The actin filaments of the larval fat body of w^{1118} cells appear to be located at the periphery of the cells as seen in Figure 16. The actin filament organization for *aur-A*^{14641} and for *aur-A*^{8839} both appear to be very similar to w^{1118} at 0 hours APF since both only have phalloidin staining, in red, at the edges of the cells as seen in Figures 17 and 18.

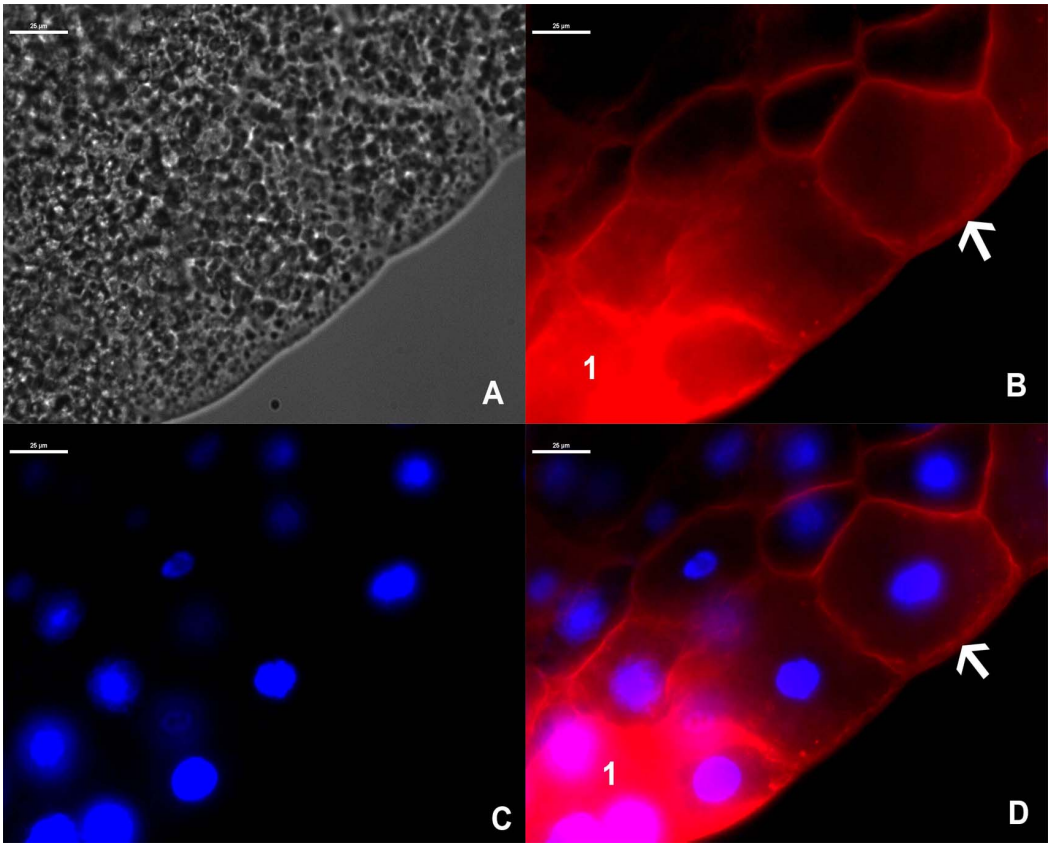

Figure 17: Image of fluorescently labelled nuclei and actin filaments of *w*^{1118} larval fat body cells. *w*^{1118} fat body was dissected and isolated at 0 hours APF and imaged using two different stains. A. Larval fat body cells imaged using phase contrast. B. Fat body cells imaged using phalloidin to stain the actin filaments red. The white arrow indicates a polygonal fat body cells with the red actin filaments located at the edge of the cell membrane giving the cell its distinct shape. C. Larval fat body imaged using DAPI to stain the nuclei blue. D. overlay of the DAPI and phalloidin images. Here the white arrow shows a polygonal larval fat body cell with its actin filaments located at the perifery of the cell with the nucleus located in the middle of the cell. The number 1 in images B and D show that this region is over-fluorescing due to an overlapping of the larval fat body tissue.

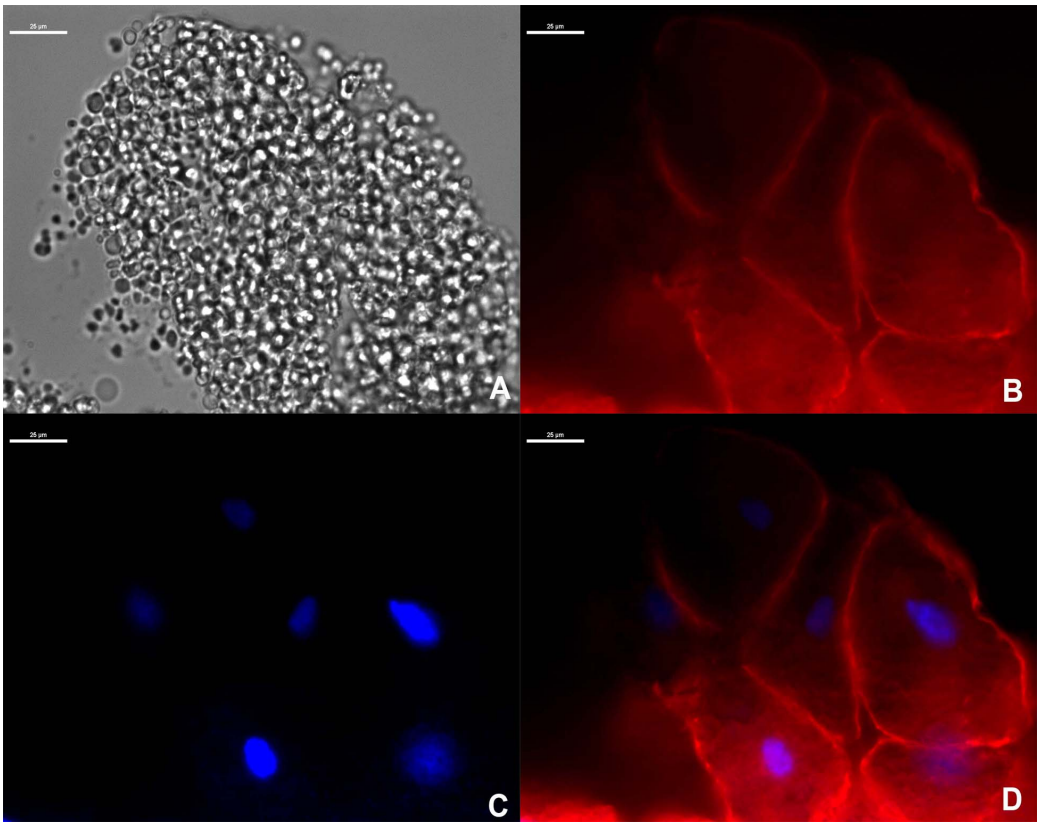

Figure 18: Image of fluorescently labelled nuclei and actin filaments of *aur-A^{8839}* larval fat body cells. *aur-A^{8839}* fat body was dissected and isolated at 0 hours APF and imaged using two different stains. A. Larval fat body cells imaged using phase contrast. B. Fat body cells imaged using phalloidin that stains the actin filaments red. C. Larval fat body imaged using DAPI to stain the nuclei blue. D. This overlay of the DAPI and phalloidin images shows that, similar to the wild-type, the actin filaments are located at the periphery of the polygonal cell with the nucleus located at the center of the cell.

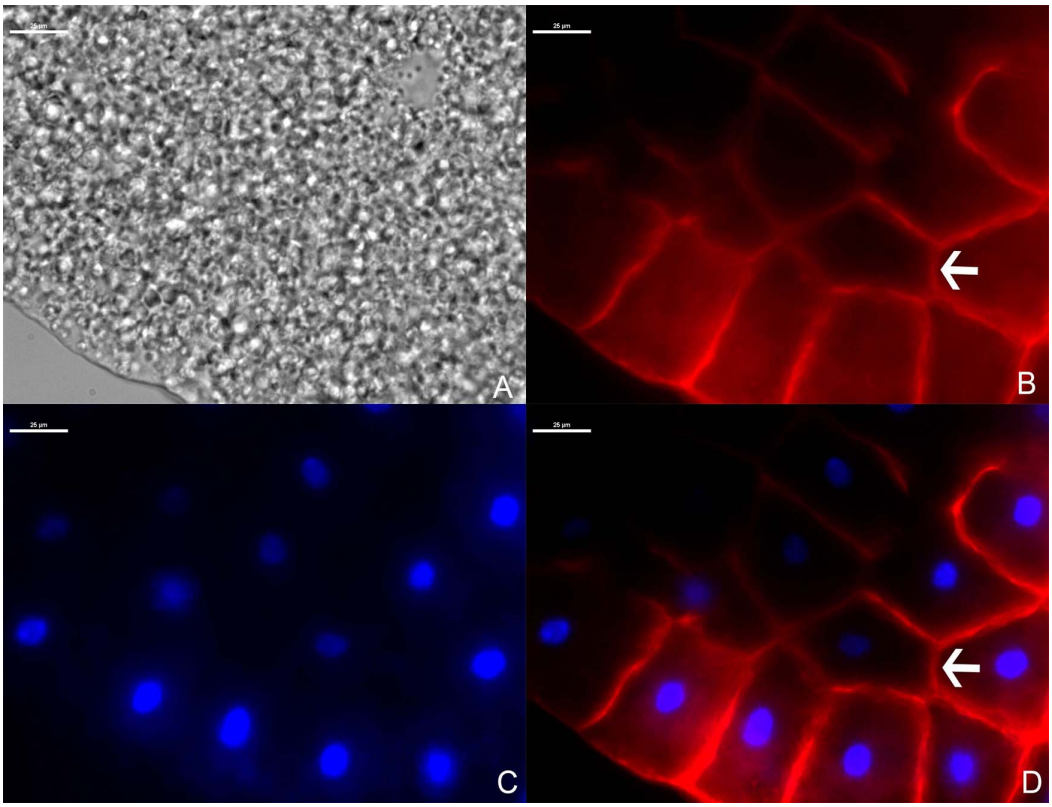

Figure 19: Image of fluorescently labelled nuclei and actin filaments of *aur-A^{14641}* larval fat body cells. *aur-A^{14641}* fat body was dissected and isolated at 0 hours APF and imaged using two different stains. A. Larval fat body cells imaged using phase contrast. B. Fat body cells imaged using phalloidin that stains the actin filaments red. The white arrow shows a polygonal cell with its actin filaments located at the edges of the cell; similar to the wild-type. C. Larval fat body imaged using DAPI to stain the nuclei blue. D. An overlay of the DAPI and phalloidin images. The white arrow in this image shows the same cells as in part B but the centrally located nucleus and the actin filaments at the cell's periphery are both visible. Scale bar indicates 25um.

This experiment was repeated at 10 hours APF to determine if there were any changes in the actin filament organization further into metamorphosis. Instead of the actin filaments being located at the periphery of the cell, the actin filaments appeared to be more centrally located. The shape of the larval fat body cells have

also changed as can be seen in Figure 19. Instead of the polygonal shape seen at 0 hours APF, the larval fat body cell is round and separated from all the other larval fat body cells. This is expected since fat body remodeling has already started at 10 hours APF. Also, some of the actin filaments remain at the periphery of the cell but there also seems to be a large amount of red fluorescence in the middle of the cell.

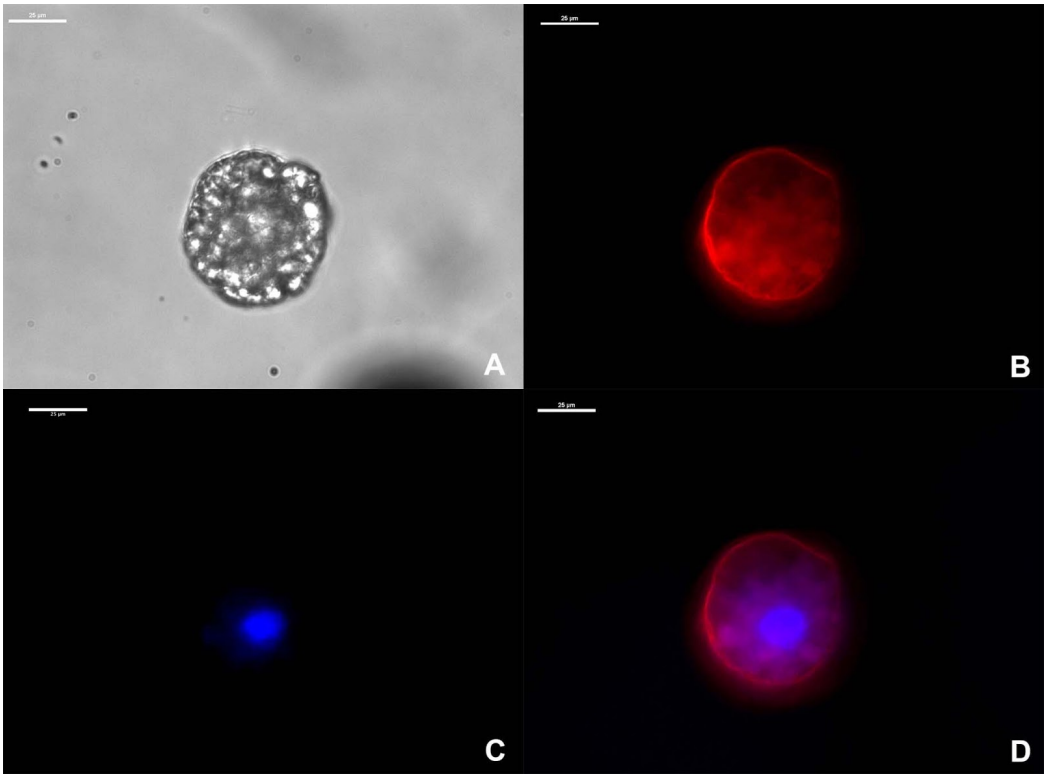

Figure 20: wild-type w^{1118} larval fat body cell imaged at 10 hours APF with fluorescently labelled nuclei and actin filaments. W^{1118} flies were isolated at 0 hours APF, the larval fat body was then dissected at 10 hours APF and imaged using phalloidin and DAPI. A. Larval fat body cells imaged using phase contrast. B. Fat body cells imaged using phalloidin that stains the actin filaments red. C. Larval fat body imaged using DAPI to stain the nuclei blue. D. An overlay of the DAPI and phalloidin images. Scale bar indicates 25um.

The larval fat body of the mutant fly lines appear different compared to the wild-type. The actin filaments are located more at the periphery of the cell but there is also a presence of actin in the center of the cell. This change in actin organization and the rounding of the cells is similar to the wild-type. However, the mutant cells have remained in groups of cells and have failed to separate from each other as can be seen in Figures 20 and 21.

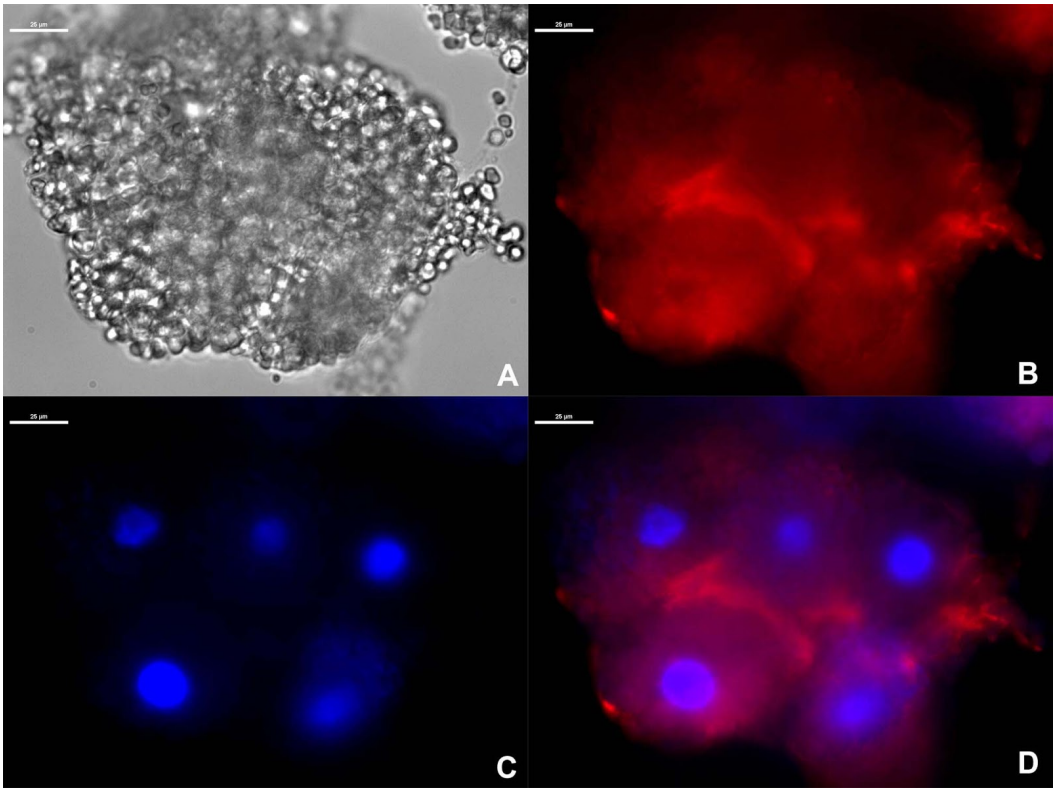

Figure 21: *aur-A*^{8839} mutant larval fat body cells imaged at 10 hours APF with fluorescently labelled nuclei and actin filaments. These mutant flies were isolated at 0 hours APF, the larval fat body was dissected at 10 hours APF and imaged using phalloidin and DAPI. A. Larval fat body cells imaged using phase contrast. B. Fat body cells imaged using phalloidin to stain the actin filaments red. C. Larval fat body imaged using DAPI to stain the nuclei blue. D. An overlay of the DAPI and phalloidin images. Scale bar indicates 25um.

The *aur-A*^{8839} mutant appears to have a strong actin filament presence on the edge of the larval fat body cells, especially where the cells are in contact with other fat body cells, as can be seen in Figure 20. However, there is a presence of some actin filaments at the center of the cell. These cells have also changed from a polygonal shape to a more spherical one.

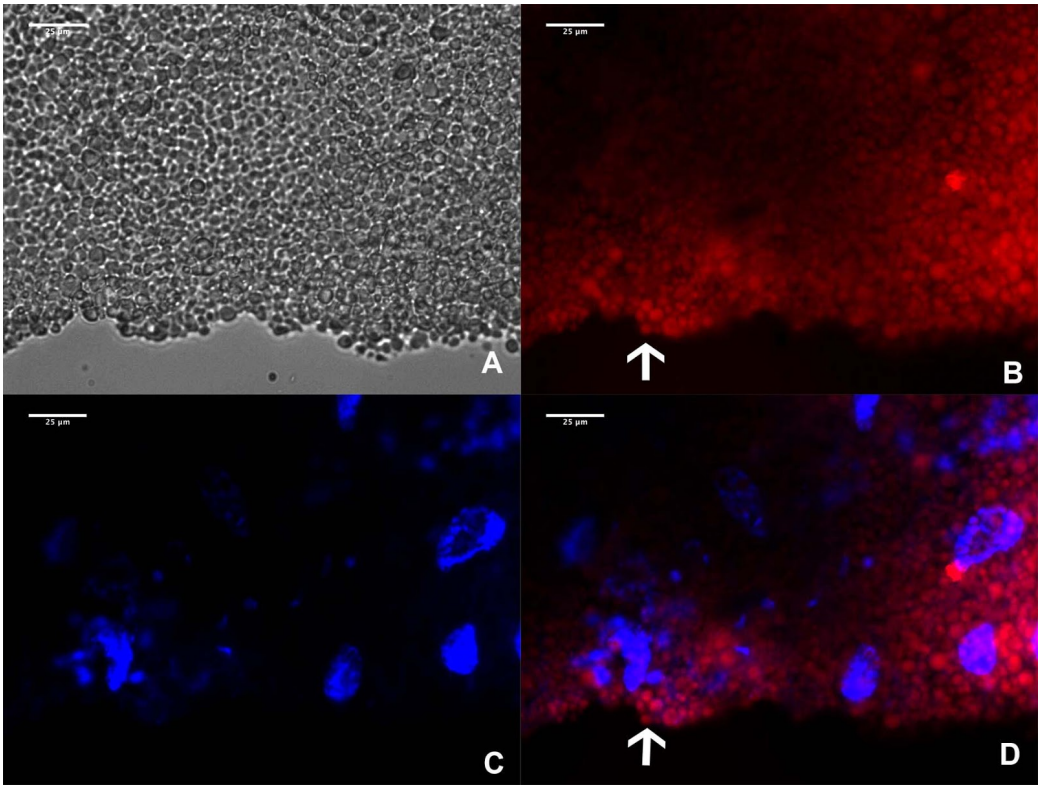

Figure 22: *aur-A*^{14641} mutant larval fat body cells imaged at 10 hours APF with fluorescently labelled nuclei and actin filaments. These mutant flies were isolated at 0 hours APF, the larval fat body was dissected at 10 hours APF and imaged using phalloidin and DAPI. A. Larval fat body cells imaged using phase contrast. B. Fat body cells imaged using phalloidin to stain the actin filaments red. C. Larval fat body imaged using DAPI to stain the nuclei blue. D. An overlay of the DAPI and phalloidin images. In part B and D, the white arrows indicate a packet of un-polymerized actin in the form of a sphere most likely because it is located in a vesicle. Scale bar indicates 25um.

The appearance of the *aur-A*^{14641} mutant larval fat body cells is very similar to that of the *aur-A*^{8839} mutant with the unseparated cells. The actin filaments are no longer located at the periphery of the cells but are in vesicles as can be seen in Figure 21 with the round red dots. The actin cytoskeleton seems to be even more perturbed than that of the *aur-A*^{8839} mutant. The appearance of the *aur-A*^{14641} mutant is comparable to that of cells undergoing programmed cell death. In both mutants, the larval fat body cells have not separated from each other.

DISCUSSION

Categorization:

Through larval fat body dissections at 12 and 14 hours APF, it was determined that many of the pharate adult lethal lines from the initial EMS mutagenesis, performed by Wang *et al*., also have abnormalities in larval fat body remodeling (Wang *et al*., 2008). The abnormalities in larval fat body remodeling were determined by identifying the presence of clumps of fat body composed of polygonal or round fat body cells. The polygonal cells indicate that remodeling has not occurred on the level of the cell's cytoskeleton. The round cells indicate that the cell is prepared for remodeling but that the ECM has not been cleaved thereby preventing cell separation and the completion of the remodeling process. The necessity of proper larval fat body remodeling for the completion of metamorphosis and eclosion is demonstrated by the pharate adult lethal lines that all have difficulty with fat body remodeling. Since metamorphosis involves multiple steps and signaling molecules, there are many reasons why improper fat body remodeling can occur.

There are a number of genes involved in larval fat body remodeling that could be mutated in any of the mutant lines. If a mutated gene affects the synthesis of 20-hydrozyecdysone (20E) steroid hormone is important to consider due to the hormone's widespread signaling that induces tissue specific cascades of gene expression that control developmental changes at specific developmental

times (Riddiford & Truman, 1993). 20E is necessary for metamorphosis and is sufficient to induce programmed cell death and puparium formation (Bond *et al.*, 2011). It has already been determined that if the titer of ecdysone is too low then metamorphosis will stop resulting in a global block in development (Cherbas *et al.*, 2003). For the larval fat body this means that if the titer of 20E is disturbed then the larval fat body is unable to remodel properly since the fat cells fail to dissociate and instead form aggregates (Bond *et al.*, 2011). In the categorized mutant lines, the cells of the larval fat body fail to separate which is normally induced by 20E. 20E is also responsible for inducing cell morphology changes during metamorphosis (Bond *et al.*, 2011). While this is not a frequent problem in the mutated *Drosophila* lines, it is present and an important characteristic of the causal mutation.

Another important gene to consider is *βftz-F1* because it is located on the third chromosome and if mutated could result in larval fat body abnormalities similar to what has been seen in this genetic screen. βFTZ-F1 is also sufficient to cause fat body remodeling during metamorphosis because matrix metalloproteinase 2 (MMP2) is a downstream target protease that cleaves the ECM. βFTZ-F1 also induces the expression of *E93* which is also located on the third chromosome, is necessary for the induction of the late cell death genes, and displays incomplete remodeling at 12 hours APF if mutated which is a possibility in this screen (Lam, 2012; Lee *et al.*, 2002).

MMP1 and MMP2 are necessary to cleave the cell-cell junctions and the basement cell membrane of the ECM and must work cooperatively to allow the cells of the larval fat body to separate (Jia *et al.*, 2014). Therefore both proteins are important to consider when contemplating problems in fat body remodeling. TIMP is located on the third chromosome and is a protein that directly inhibits the function of MMP1 and MMP2 (Wei *et al.*, 2003). If TIMP has been altered by the random mutagenesis it is possible that MMP1 and MMP2 activity is negatively impacted resulting in the inability of the larval fat body to remodel properly.

Finally, dILP, dInR, PI3K and AKT are located on the third chromosome and potential targets for the random EMS mutagenesis. The PI3K pathway involves the previously mentioned proteins that are important for growth and metabolism. Insulin-like Peptide (dILP) has a similar function to Insulin-like Growth Factor (IGF) in mammals and forms a complex with the insulin receptor (dInR) to initiate a phosphorylation cascade that uses phosphoinositide 3-kinase (PI3K) to activate Target of Rapamycin (TOR) (Li *et al.*, 2010). If mutated, insulin signaling could be disrupted which would result in abnormal fat body remodeling.

Complementation tests:

Complementation tests were performed to determine the number of genes involved in the no remodeling phenotype. Each of the no remodeling lines was crossed to the other and the progeny of this cross was examined for abnormal

remodeling. If there was abnormal larval fat body remodeling observed in the progeny, then there was no wild type gene in the progeny to supply a functional protein because the mutations in the original parental lines affect the same gene. This does not mean that the two lines have the same mutation, only that the same gene is affected. If wild-type larval fat body remodeling is observed, then there is a wild-type copy of the gene that produces a functional protein because the two original mutations in the parental lines affect two different genes.

Wild-type remodeling and pharate adult lethality were not observed in the crosses that were performed. According to the hypothesis that abnormalities in larval fat body remodeling cause pharate adult lethality due to a lack of energy for the fully formed adult flies to escape their pupal case, these results seem inconsistent. There were various levels of partial remodeling in the progeny that seems to allow just enough remodeling for the adult fly to eclose. Since the flies are kept in vials full of food, the newly eclosed adult can easily find and access the food to provide energy for survival after eclosion. A colleague examined the survival of the progeny after they had eclosed in an environment with no food. The wild-type flies live for three days but preliminary data suggests the progeny from the complementation tests are unable to supply enough energy to survive these three days post-eclosion. This indicates that the defects in remodeling allow for eclosion but are unable to fuel the survival of the adult flies for as long as the wild-type adults do (Levy, unpublished).

One hypothesis when interpreting these results is that there are seven different mutated genes, one in each of the no remodeling lines, that all participate in the same biochemical pathway. If one gene only has one wild-type copy that produces half the amount of functional protein, then there will be difficulty producing the same amount of product that is necessary for the next step in the biochemical pathway. This difficulty is only compounded with the addition of another gene being mutated at another site. If this is true, this could explain why there are various amounts of partial remodeling observed in the progeny that are able to eclose form their pupal case.

Mapping:

Using the mapping scheme proposed by Sapiro *et al*., an estimation of the chromosomal locations of I(3)LL- 7275: L 04 PA and I(3)LL- 13567: L 04 PA were determined (Sapiro *et al.*, 2013). However, due to the limited amount of progeny obtained, the calculated position is only an estimate and is unlikely to be the precise location of the gene and its mutation. This information does allow for a smaller section of the third chromosome to be sequenced to determine the exact location and nature of the mutation as well as the gene that it affects.

As for I(3)LL- 15413: L 04 PA, the large proportion of the wild-type phenotype in the F_2 generation to be scored for each arm of the chromosome indicates that the gene is not likely to be in either region. These results suggest that this mutation is located closer to the center of the chromosome. It would be

interesting to repeat the mapping procedure but modify it to include *Gl* and *Sb* dominant markers to better determine where in the center of the chromosome the mutation is. Similar to the previous two lines, the limited amount of progeny to be scored affects the observed splits. If this experiment is to be repeated with the addition of the other two dominant markers, a larger number of F_2 progeny should be collected to be scored to obtain a more precise location for this mutation.

The final line, I(3)LL- 11075: L 04 PA, yielded inconclusive results. The number of F_2 progeny was insufficient to determine if the splits indicated that the gene was inside or outside of the *H, Pr* or the *R, D* pairs of dominant genes. This mapping experiment should be repeated on this line as well with the two additional dominant markers (*Gl* and *Sb*) to obtain more conclusive results on the chromosomal location of this gene.

Fluorescence Microscopy:

Actin filament visualization using fluorescence microscopy yielded clear images and the change in actin filament organization was informative on the role of *aur-A*. At 0 hours APF, the wild-type w^{1118} flies appeared very similar to the $aur\text{-}A^{14641}$ and $aur\text{-}A^{8839}$ mutated lines. All three had actin filaments located at the periphery of the cell, the cells were in a polygonal shape and located in a sheet. However, looking closely at the $aur\text{-}A^{8839}$ mutated line, there are small gaps between the cells. These gaps could indicate that the health of the cells in the fat body tissue is affected and the cells are starting to express defects in remodeling.

At 10 hours APF, the two mutants appear very different when compared to the wild-type cells. At this time point, the w^{1118} cells appear spherical and round which indicates proper remodeling. There are some actin filaments at the periphery but there seems to be more actin located in the center of the cell. This actin could either be filamentous, but out of the plane of focus, or could be depolymerized.

The *aur-A*^{8839} mutated line cells are still in groups of cells and have more actin located where the spherical cells connect to one another. These differences from the wild-type indicate that this mutation in *aur-A* causes defects in remodeling in the form of unseparated larval fat body cells and the increase in intracellular actin location where the cells touch. The spherical appearance of the cells indicate that these larval fat body cells are ready for remodeling but that the ECM that connects them has not been fully degraded, possibly due to the *aur-A* mutation. The health of these cells is also in question since cells that undergo cell death also appear spherical with cytoskeleton abnormalities. It would be interesting to determine if the cells are alive during metamorphosis. If these cells die, it could help explain why *aur-A*^{8839} mutants are pharate adult lethal. If the tissue is no longer alive it would be unable to provide energy for metamorphosis. Since the microtubule visualization method using fluorescence microscopy yielded no insightful data, a different type of microtubule visualization would be beneficial to determine the effects of this *aur-A* mutation.

The *aur-A*^{14641} mutated line cells are still in groups of spherical cells and have actin in globules dispersed throughout the cell. It is likely that this globular appearance of the actin is caused by it being contained in vesicles. Usually proteins in these vesicles are being degraded as seen in autophagic tissue. The nuclei of these cells also seem to be broken up, another indicator of dying tissue. Similar to the *aur-A*^{8839} mutant, it would be informative to determine the organization of the microtubules and if the larval fat body cells are alive at this point in metamorphosis.

MMP2 is a GPI anchored protein meaning that during its synthesis the gene needs to be transcribed, translated into the membrane of the endoplasmic reticulum, post translationally modified to include GPI and then transported to the cell surface using vesicle transport. It is possible that MMP2 containing vesicles are transported along actin filaments. MMP2 is only produced during metamorphosis when Aur-A seems to be affecting the organization of the actin cytoskeleton. If MMP2 is transported to the cell membrane using actin filaments that are perturbed due to mutations in the *aur-A* gene, then it is possible that an insufficient amount of MMP2 is successfully transported to the cell surface to allow wild-type remodeling. This should be explored further in future experiments.

The overall change in shape seen in the wild-type and both mutant from a polygonal to a spherical cell could be due to the change in organization of the

actin filaments. The microtubule arrangement may be participating in this change in shape but this should be studied through microtubule visualization at different points during metamorphosis.

Summary and Future Studies:

A genetic screen was conducted using EMS mutated fly strains with mutation on the third chromosome and are pharate adult lethal to attempt to identify novel genes necessary for fat body remodeling. Starting this genetic screen with the categorization of multiple mutated lines, it was determined how many mutations resulted in abnormal larval fat body remodeling phenotypes. The mutated lines were categorized into three groups depending on their level of remodeling at 12 and 14 hours APF.

With the help of complementation tests, it was determined that the no remodeling phenotype was caused by seven different genes that participate in the same biochemical pathway. With the help of the mapping, the approximate location of two genes was determined. The mapping results confirm those of the complementation test by indicating that the two mapped lines, belonging to the no remodeling phenotype, had two different mutated genes.

The mapping experiment that was performed only used 2 pairs of dominant markers: *H, Pr* and *R, D*. In the future, it would be helpful to repeat the mapping experiment with all three sets of dominant markers (*H* and *Pr, R* and *D,*

and *Gl* and *Sb*) to obtain a more precise chromosomal location for the no remodeling lines. This future experiment should also aim to increase the number of F_2 progeny to be scored and used to determine the number of splits and in the mapping location equation. These future results should confirm the results of the complementation tests by indicating that there are seven different genes involved in the no remodeling phenotype.

Once the approximate locations of the mutations have been determined, this region of the third chromosome should be sequenced to determine the nature of the mutation. Once the mutated genes have been sequences the mutation's effect on the encoded protein and what this protein's role is in fat body remodeling can be determined.

The line I(3)LL-14641: L 04 PA , also known as *aur-A*^{14641}, was mapped to the *aur-A* gene. This mutated line was determined to be in the same complementation group as *aur-A*^{17961} and *aur-A*^{8839}. The role of Aur-A in fat body remodeling has not yet been determined but through visualizing the actin at 0 hours and 10 hours APF there seems to be some defects in actin organization at 10 hours APF. The organization of the rest of the cytoskeleton should be determined perhaps with confocal microscopy and a non-green microtubule fluorescent dye. Due to the unhealthy appearance of the fat body cells in these preliminary results obtained with the actin stain, it would be helpful to determine if these cells are alive. If the larval fat body cells are not alive, then it would be

understandable why the larval fat body fails to remodel and the lack of energy that prevents the fly from eclosing. This gene's function is unclear but it seems to affect the cytoskeletal arrangement and cell health during metamorphosis.

These findings suggest that further research is needed to conclude on the nature of the randomly mutated genes in this genetic screen and the role of Aur-A in fat body remodeling during metamorphosis. The genes involved in fat body remodeling in *Drosophila melanogaster* may have homologues in humans which could aid the understanding of tissue remodeling and aid in the development of better treatment protocols for wound healing and metastasis in humans.

APPENDIX

Parental lines in the no remodeling category:

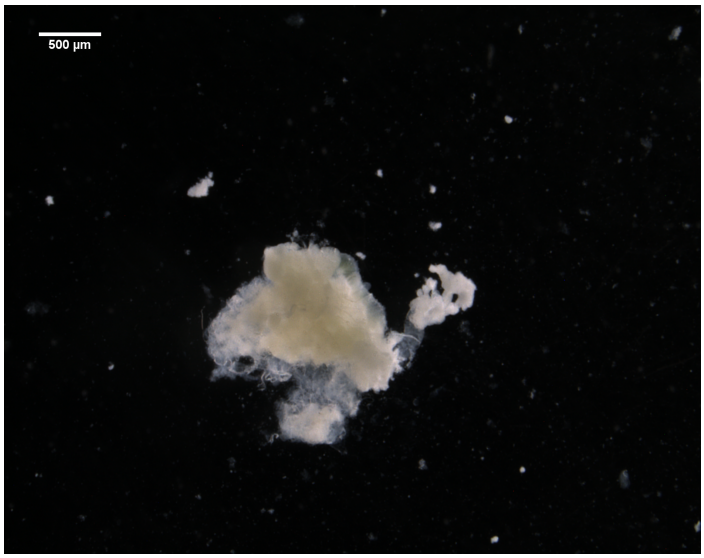

Figure 23: Homozygous I(3)LL-15413: L 04 PA mutant dissected at 12 hours APF. Categorized into the no remodeling group (Walchessen, 2016).

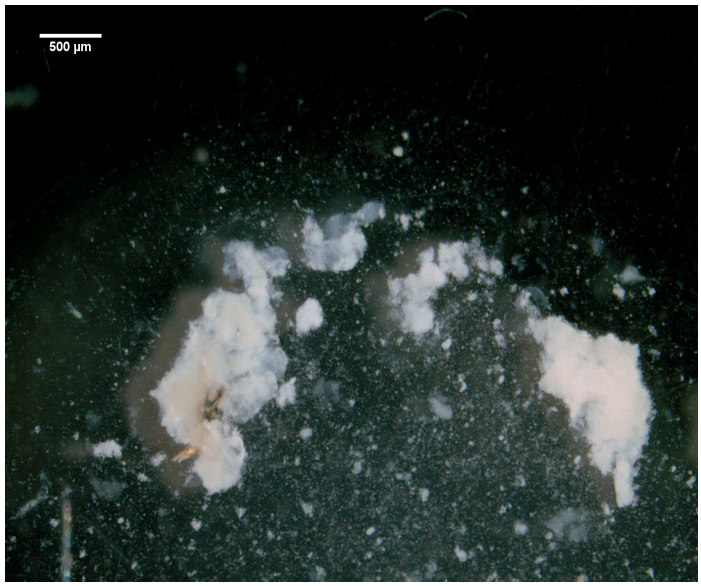

Figure 24: Homozygous I(3)LL-2310: L 04 PA mutant dissected at 12 hours APF. Categorized into the no remodeling group (Walchessen, 2016).

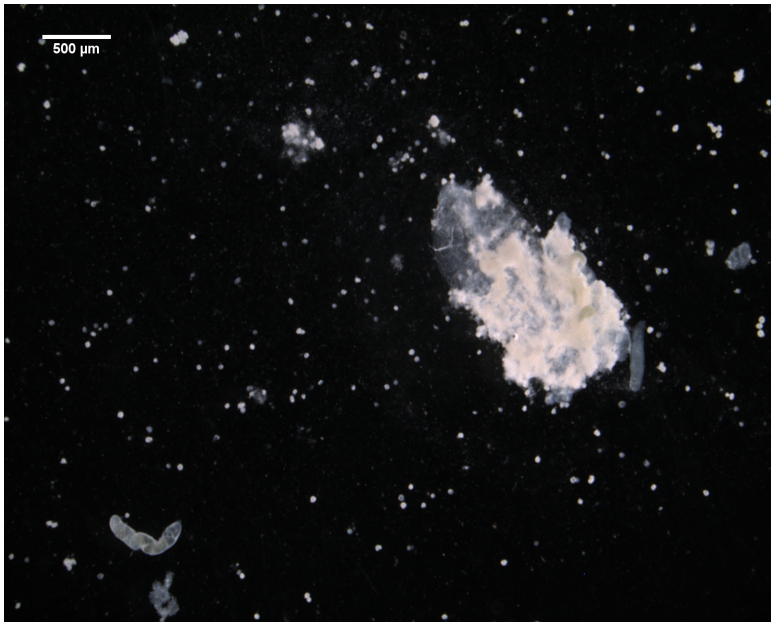

Figure 25: Homozygous I(3)LL-7275: L 04 PA mutant dissected at 12 hours APF. Categorized into the no remodeling group (Walchessen, 2016).

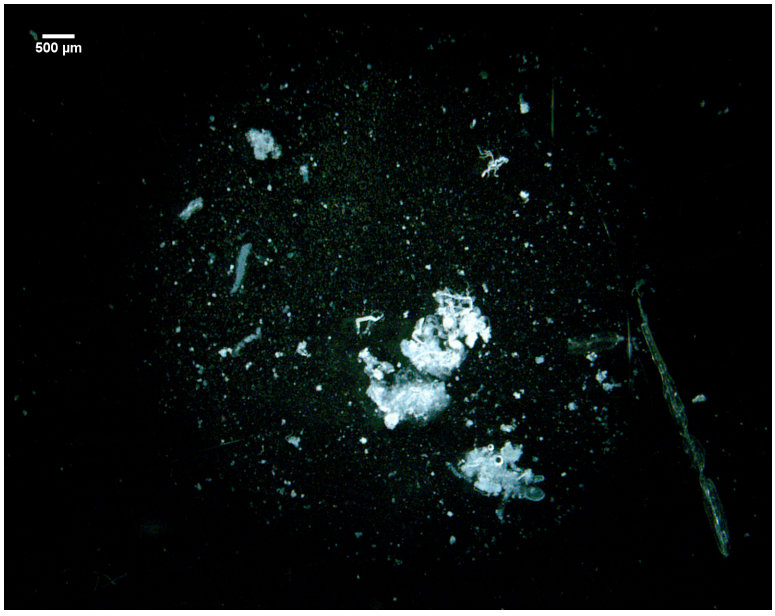

Figure 26: Homozygous I(3)LL-13567: L 04 PA mutant dissected at 12 hours APF. Categorized into the no remodeling group (Walchessen, 2016).

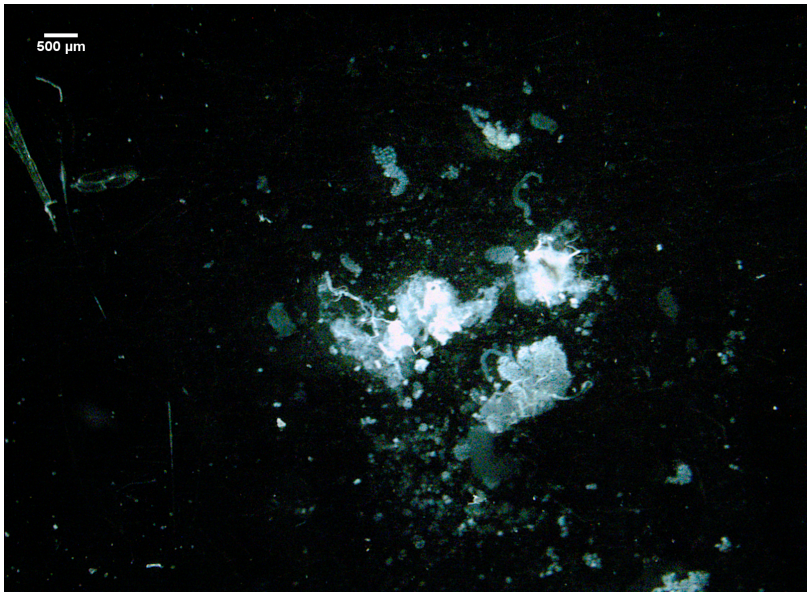

Figure 27: Homozygous I(3)LL-15370: L 04 PA mutant dissected at 12 hours APF. Categorized into the no remodeling group (Walchessen, 2016).

Complementation tests:

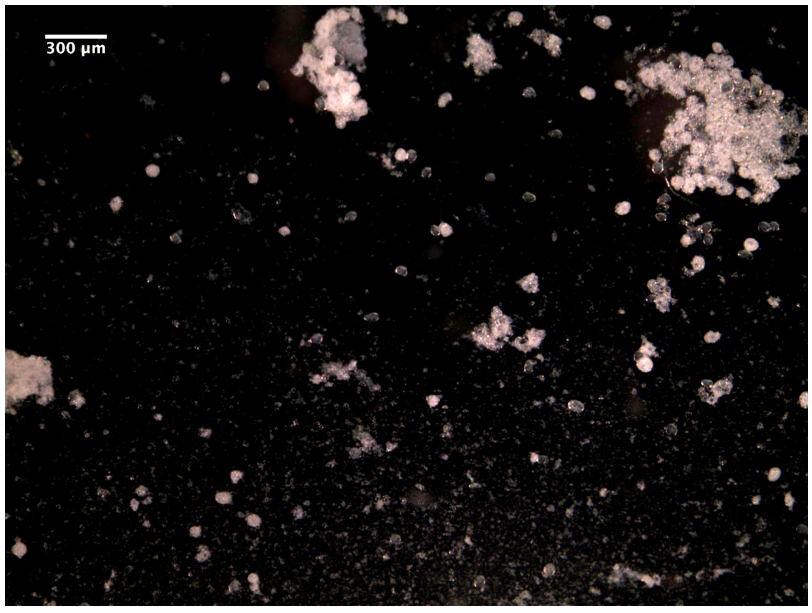

Figure 28: Progeny dissection of the I(3)LL-13567: L 04 PA x I(3)LL-17770: L 04 PA mutant cross at 14 hours APF. Categorized as partial remodeling.

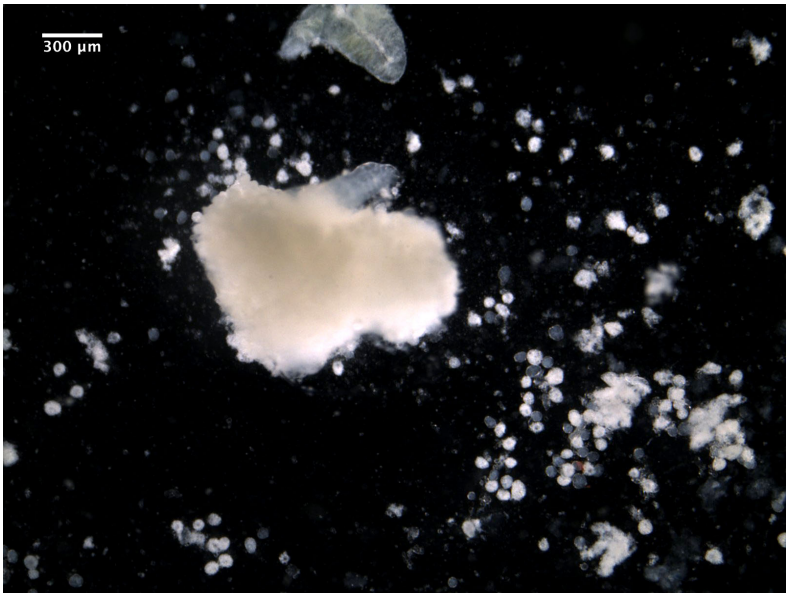

Figure 29: Progeny dissection of the I(3)LL-15413: L 04 PA x I(3)LL-13567: L 04 PA mutant cross at 14 hours APF. Categorized as partial remodeling.

Figure 30: Progeny dissection of the I(3)LL-15413: L 04 PA x I(3)LL-11075: L 04 PA mutant cross at 14 hours APF. Categorized as partial remodeling.

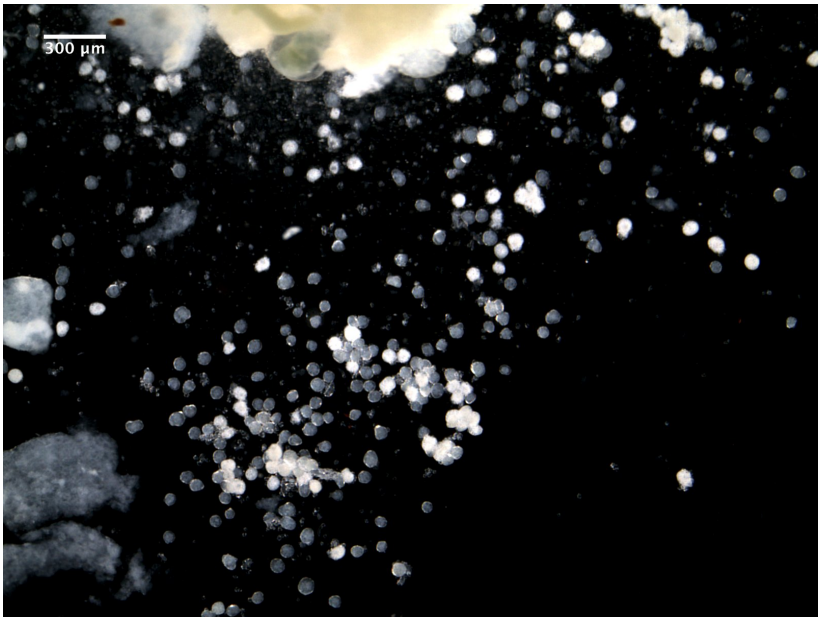

Figure 31: Progeny dissection of the I(3)LL-17770: L 04 PA x I(3)LL-7275: L 04 PA mutant cross at 14 hours APF. Categorized as partial remodeling.

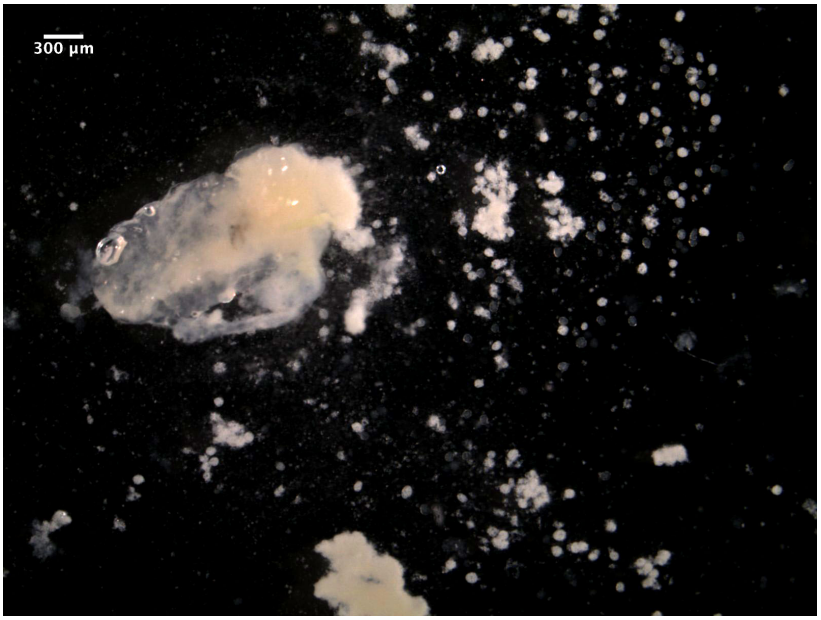

Figure 32: Progeny dissection of the I(3)LL-17770: L 04 PA x I(3)LL-11075: L 04 PA mutant cross at 14 hours APF. Categorized as partial remodeling.

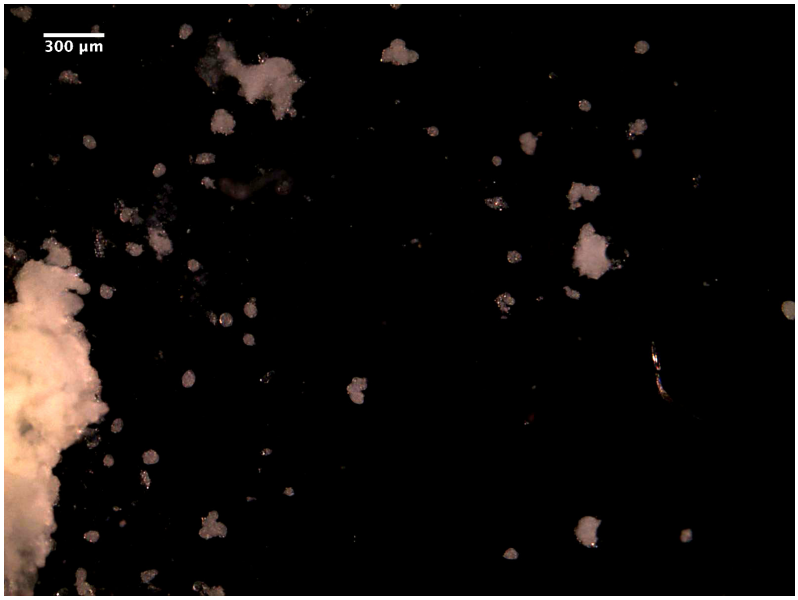

Figure 33: Progeny dissection of the I(3)LL-17770: L 04 PA x I(3)LL-13567: L 04 PA mutant cross at 14 hours APF. Categorized as partial remodeling.

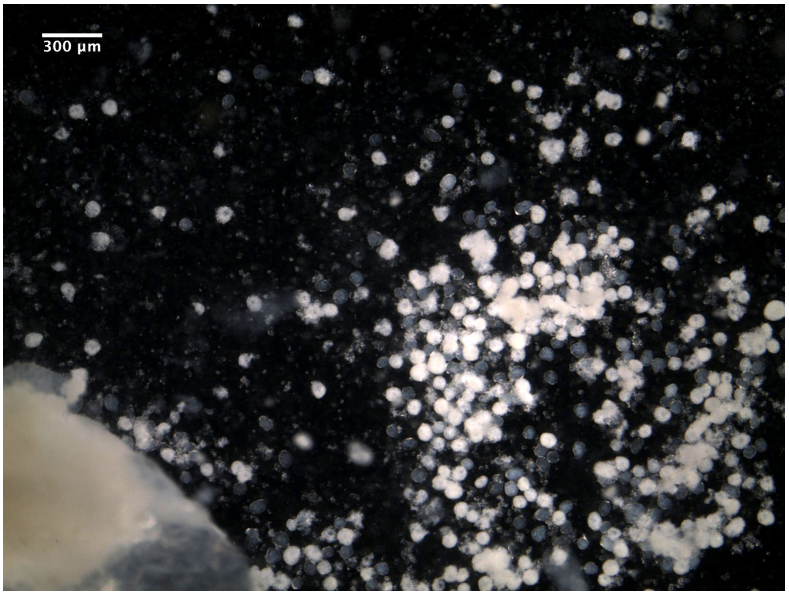

Figure 34: Progeny dissection of the I(3)LL-2310: L 04 PA x I(3)LL-17770: L 04 PA mutant cross at 14 hours APF. Categorized as partial remodeling.

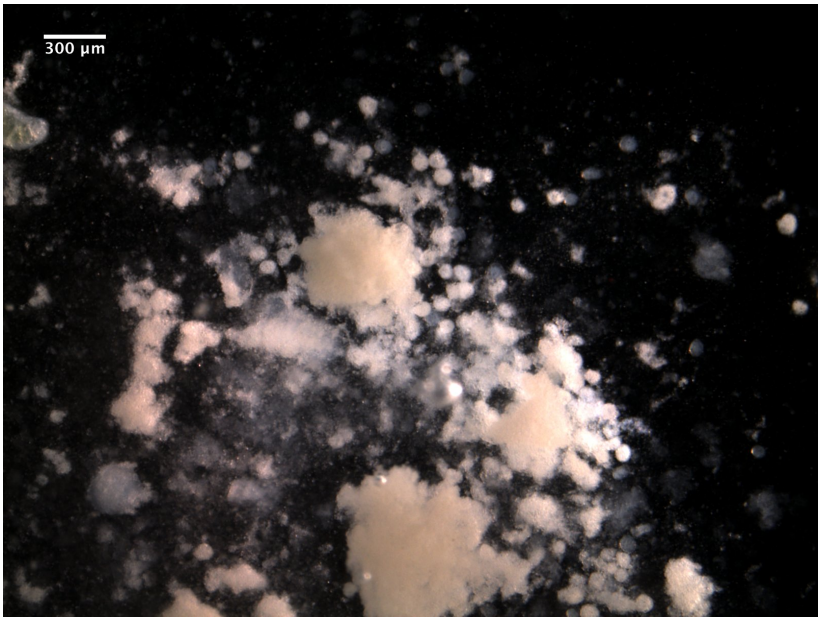

Figure 35: Progeny dissection of the I(3)LL-2310: L 04 PA x I(3)LL-7275: L 04 PA mutant cross at 14 hours APF. Categorized as partial remodeling.

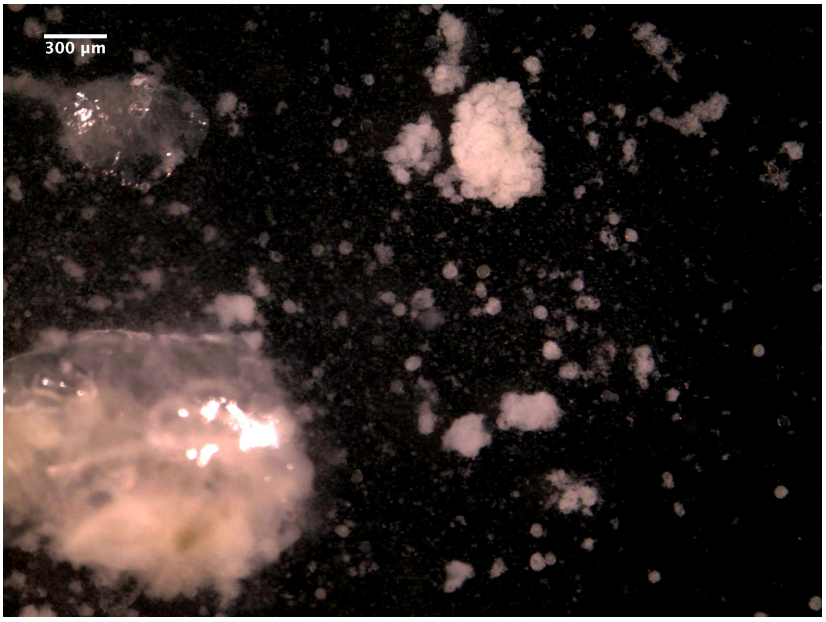

Figure 36: Progeny dissection of the I(3)LL-2310: L 04 PA x I(3)LL-13567: L 04 PA mutant cross at 14 hours APF. Categorized as partial remodeling.

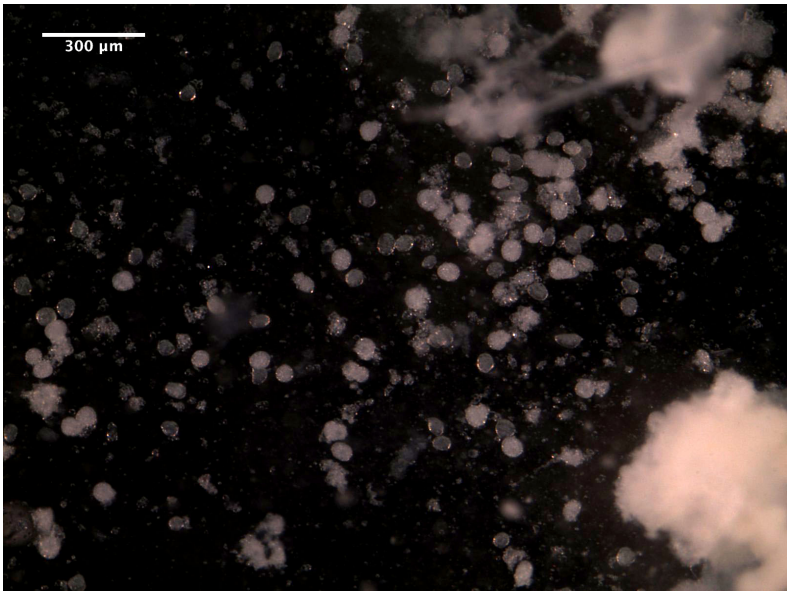

Figure 37: Progeny dissection of the I(3)LL-2310: L 04 PA x I(3)LL-15413: L 04 PA mutant cross at 14 hours APF. Categorized as partial remodeling.

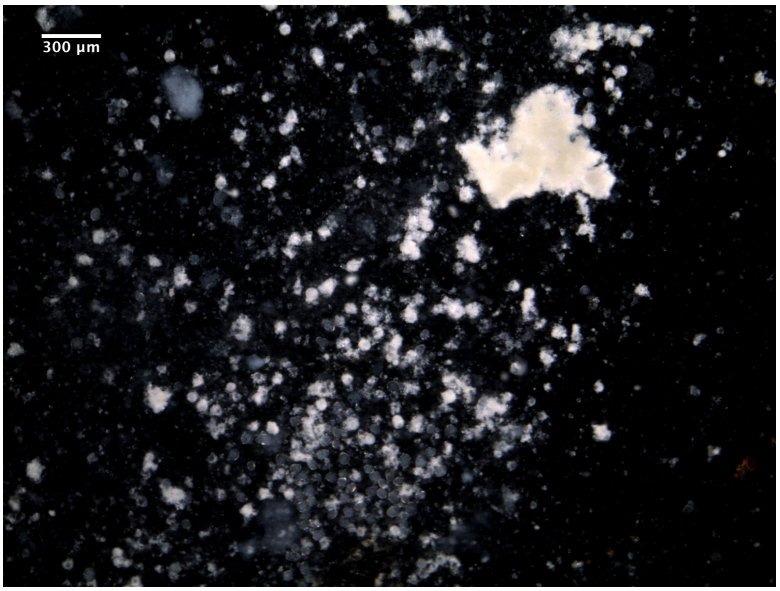

Figure 38: Progeny dissection of the I(3)LL-7275: L 04 PA x I(3)LL-11075: L 04 PA mutant cross at 14 hours APF. Categorized as partial remodeling.

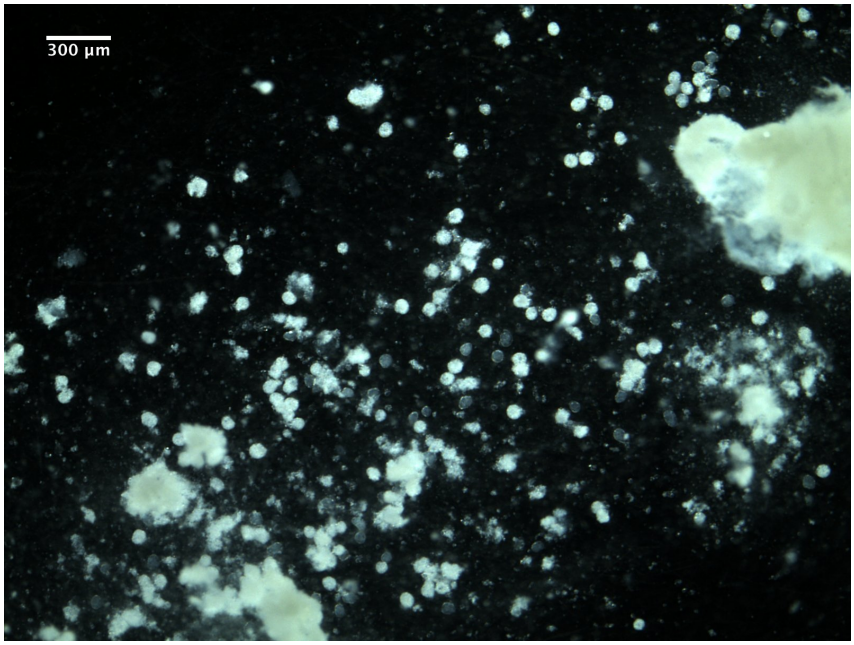

Figure 39: Progeny dissection of the I(3)LL-7275: L 04 PA x I(3)LL-15241: L 04 PA mutant cross at 14 hours APF. Categorized as partial remodeling.

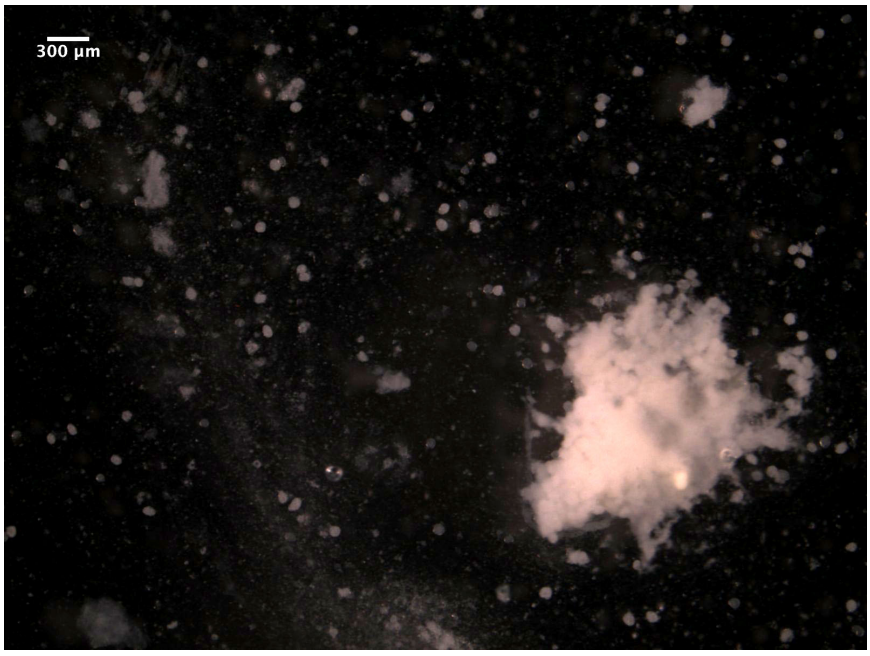

Figure 40: Progeny dissection of the I(3)LL-7275: L 04 PA x I(3)LL-2310: L 04 PA mutant cross at 14 hours APF. Categorized as partial remodeling.

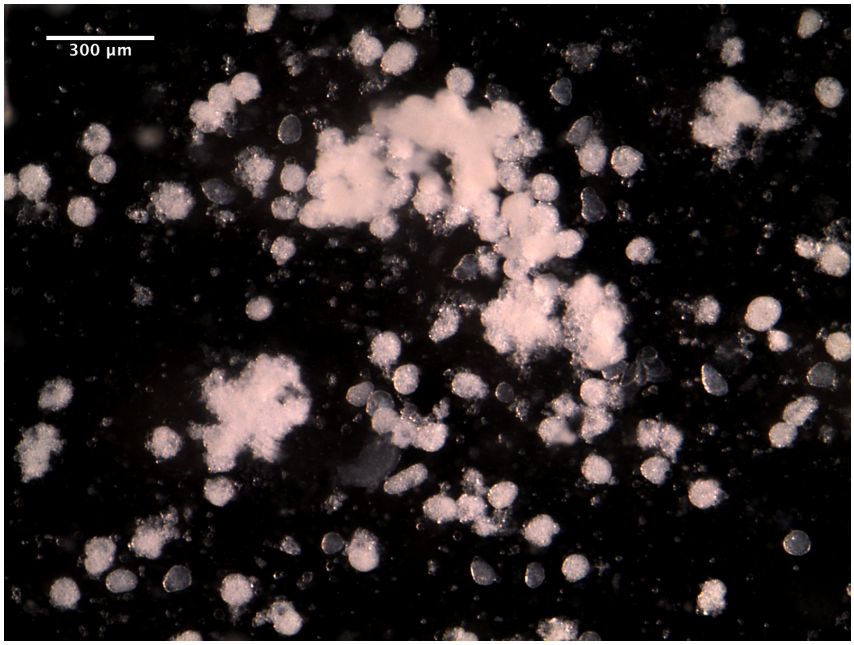

Figure 41: Progeny dissection of the I(3)LL-11075: L 04 PA x I(3)LL-2310: L 04 PA mutant cross at 14 hours APF. Categorized as partial remodeling.

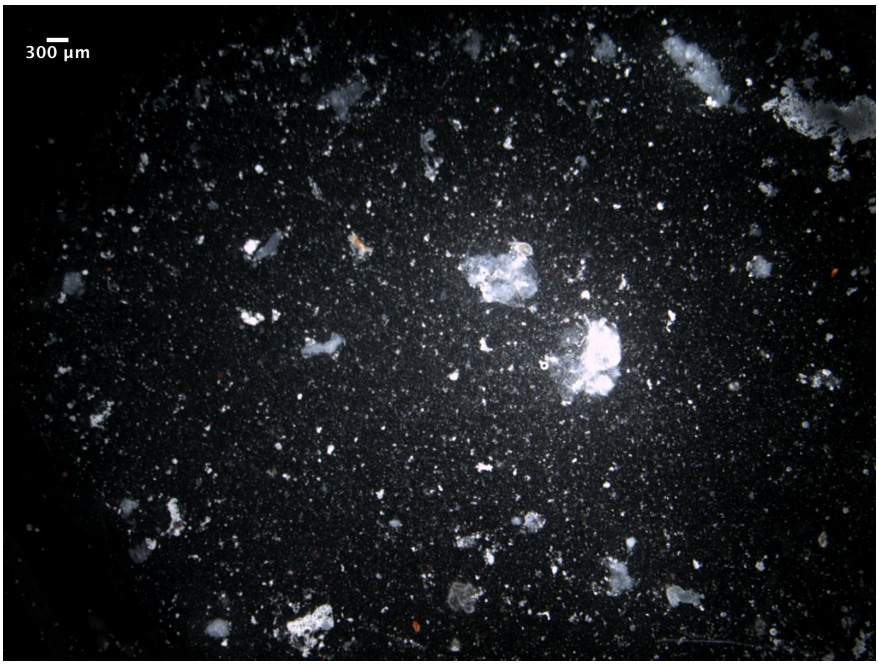

Figure 42: Progeny dissection of the I(3)LL-11075: L 04 PA x I(3)LL-13567: L 04 PA mutant cross at 14 hours APF. Categorized as partial remodeling.

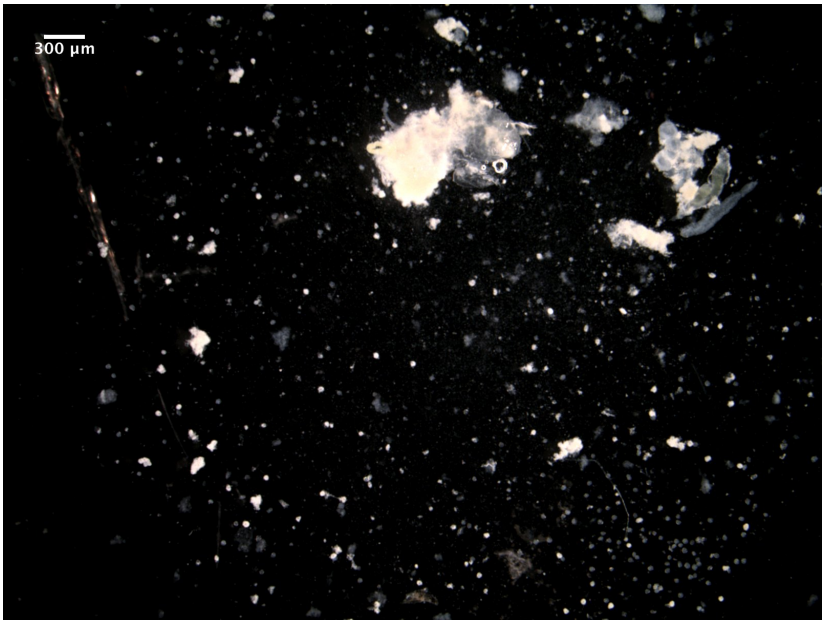

Figure 43: Progeny dissection of the I(3)LL-13567: L 04 PA x I(3)LL-11075: L 04 PA mutant cross at 14 hours APF. Categorized as partial remodeling.

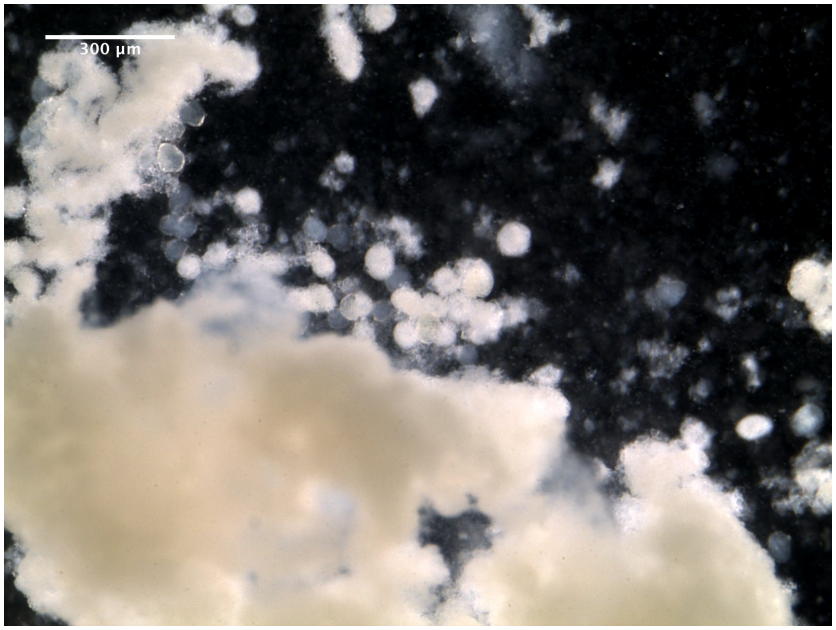

Figure 44: Progeny dissection of the I(3)LL-13567: L 04 PA x I(3)LL-2310: L 04 PA mutant cross at 14 hours APF. Categorized as partial remodeling.

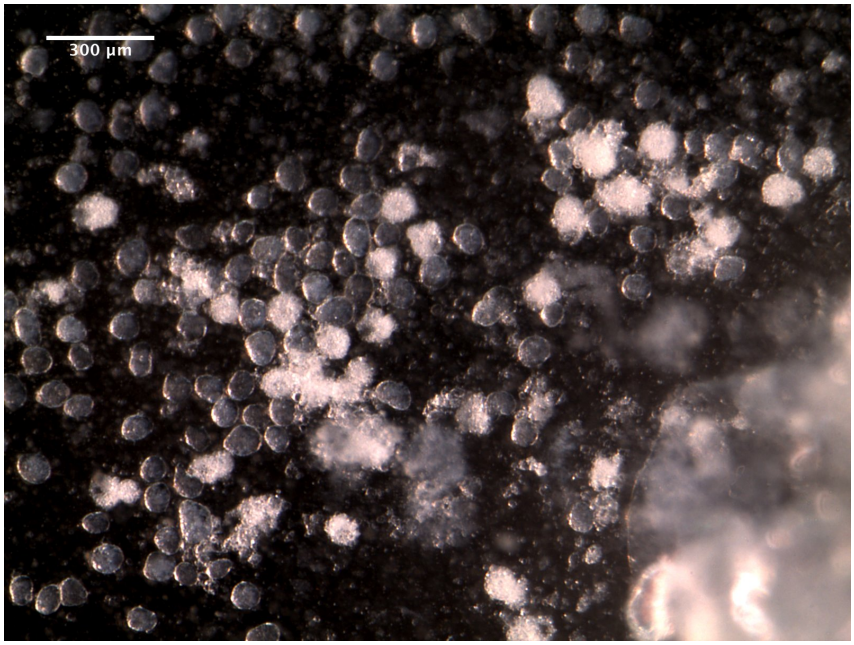

Figure 45: Progeny dissection of the I(3)LL-15413: L 04 PA x I(3)LL-7275: L 04 PA mutant cross at 14 hours APF. Categorized as partial remodeling.

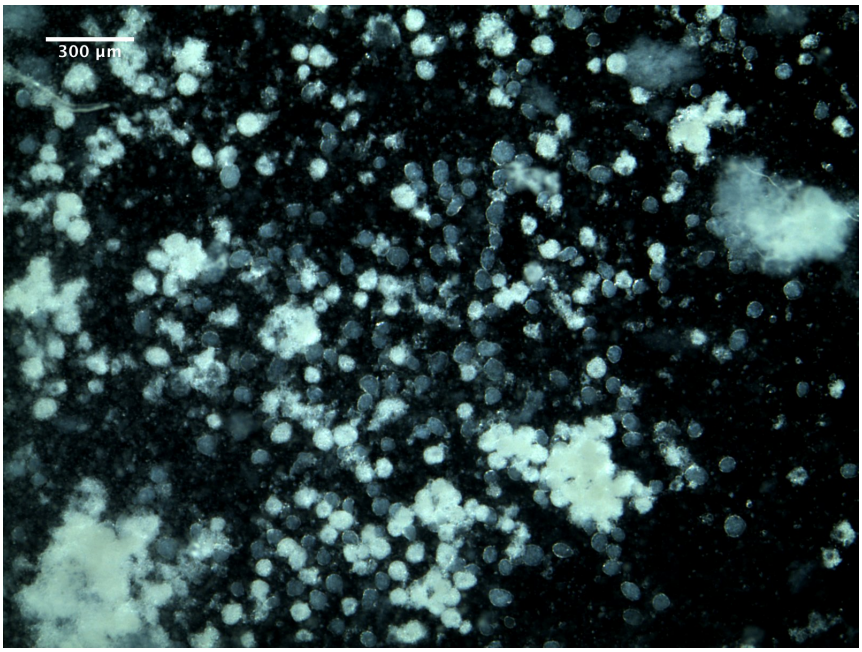

Figure 46: Progeny dissection of the I(3)LL-7275: L 04 PA x I(3)LL-13567: L 04 PA mutant cross at 14 hours APF. Categorized as partial remodeling.

Mapping:

Equation 2: Map position of I(3)LL-7275: L 04 PA in cM (Sapiro et al., 2013)

$$= \frac{(loss\ of\ left\ marker)}{(loss\ of\ left\ marker) + (loss\ of\ right\ marker)} \times (cM\ between\ markers) + (cM\ of\ left\ marker)$$

$$= \frac{71}{71+54} \times 20.5cM + 69.5cM = 81.14cM$$

Equation 3: *Map position of* 13567 *in cM* (Sapiro et al., 2013)

$$= \frac{(loss\ of\ left\ marker)}{(loss\ of\ left\ marker) + (loss\ of\ right\ marker)} \times (cM\ between\ markers) + (cM\ of\ left\ marker)$$

$$= \frac{63}{63+24} \times 39.3cM + 1.4cM = 29.8586cM$$

LITERATURE CITED

Adams, M. D., Celniker, S. E., Holt, R. A., Evans, C. A., Gocayne, J. D., Amanatides, P. G., … Venter, J. C. (2000). The Genome Sequence of Drosophila melanogaster. *Science*, *287*, 2185–2195.

Aguila, J. R., Suszko, J., Gibbs, A. G., & Hoshizaki, D. K. (2007). The role of larval fat cells in adult Drosophila melanogaster. *The Journal of Experimental Biology*, *210*, 956–963.

Bond, N. D., Nelliot, A., Bernardo, M. K., Ayerh, M. A., Gorski, K. A., Hoshizaki, D. K., & Woodard, C. T. (2011). Author's personal copy ßFTZ-F1 and Matrix metalloproteinase 2 are required for fat-body remodeling in Drosophila. *Developmental Biology*, *360*, 286– 296. Retrieved from http://www.elsevier.com/copyright

Cherbas, L., Hu, X., Zhimulev, I., Belyaeva, E., & Cherbas, P. (2003). EcR isoforms in Drosophila : testing tissue-specific requirements by targeted blockade and rescue. *Development*, *130*, 271–284. http://doi.org/10.1242/dev.00205

Cowin, S. C. (2004). TISSUE GROWTH AND REMODELING. *Annu. Rev. Biomed. Eng*, *6*, 77–107. http://doi.org/10.1146/annurev.bioeng.6.040803.140250

Cox, T. R., & Erler, J. T. (2011). Remodeling and homeostasis of the extracellular matrix: implications for fibrotic diseases and cancer. *Disease Models & Mechanisms*, *4*(2), 165–78. http://doi.org/10.1242/dmm.004077

Cytoskeleton Inc. (n.d.). *Datasheet - Rhodamine Phalloidin*. Retrieved from http://www.cytoskeleton.com/pdf-storage/datasheets/phdr1.pdf

Gausz, J., Gyurkovics, H., Bencze, G., Awad, A. A. M., Holden, J. ., & Ish-Horowics, D. (1981). Genetic Characterization of the Region Between 86F1,2 and 87B15 on Chromosome 3 of Drosophila melanogaster. *Genetics*, *98*, 775–789.

Hacker, U., Grossniklaus, U., Gehring, W., & Jackle, H. (1992). Developmentally Regulated Drosophila Gene Family Encoding the Fork Head Domain. *Developmental Biology*, *89*, 8754–8758.

Herboso, L., Oliveira, M. M., Talamillo, A., Pérez, C., González, M., Martín, D., … Barrio, R. (2015). Ecdysone promotes growth of imaginal discs through the regulation of Thor in D. melanogaster. http://doi.org/10.1038/srep12383

Hoshizaki, D. K. (2005). Fat-Cell Development. In *Fat-Cell Development*. Las Vegas: Elsevier.

Hoskins, R. A., Phan, A. C., Naeemuddin, M., Mapa, F. A., Ruddy, D. A., Ryan, J. J., … Ellis, M. C. (2001). Single nucleotide polymorphism markers for genetic mapping in Drosophila melanogaster. *Genome Research*, *11*, 1100–1113. http://doi.org/10.1101/gr.178001

Jennings, B. H. (2011). Drosophila-- a versatile model in biology & medicine. *Materials Today*, *14*(5), 190–195. http://doi.org/10.1016/S1369-

7021(11)70113-4

Jia, Q., Liu, Y., Liu, H., & Li, S. (2014). Mmp1 and Mmp2 cooperatively induce Drosophila fat body cell dissociation with distinct roles. *SCIENTIFIC REPORTS*, *4*(7535), 1–12. http://doi.org/10.1038/srep07535

King-Jones, K., Charles, J. P., Lam, G., & Thummel, C. S. (2005). The ecdysone-induced DHR4 orphan nuclear receptor coordinates growth and maturation in Drosophila. *Cell*, *121*, 773–784. http://doi.org/10.1016/j.cell.2005.03.030

Kuman, V., Abbas, A. K., & Aster, J. C. (2014). Robbins & Cotran Pathologic Basis of Disease. In *Robbins & Cotran Pathologic Basis of Disease* (Fourth, pp. 69–112). Philadelphia: Saunders.

Lam, W. Y. (2012). *The role of E93 in Fat Body Remodeling in Drosophila melanogaster.* Mount Holyoke College.

Lee, C.-Y., Simon, Claudia, R., Woodard, C. T., & Baechrecke, Eric, H. (2002). Genetic Mechanism for the Stage - and Tissue - Specific Regulation of Steroid Triggered Programmed Cell Death in Drosophila. *Development (Cambridge, England)*, *252*, 138–148.

Lee, C. Y., Andersen, R. O., Cabernard, C., Manning, L., Tran, K. D., Lanskey, M. J., … Doe, C. Q. (2006). Drosophila Aurora-A kinase inhibits neuroblast self-renewal by regulating aPKC/Numb cortical polarity and spindle orientation. *Genes and Development*, *20*, 3464–3474. http://doi.org/10.1101/gad.1489406

Li, Y., Ray, P., Rao, E. J., Shi, C., Guo, W., Chen, X., … Wang, X. (2010). A Drosophila model for TDP-43 proteinopathy. *Pnas*, *107*(7), 3169–3174. http://doi.org/10.1073/pnas.0913602107

Moon, W., & Matsuzaki, F. (2013). Aurora A kinase negatively regulates Rho-kinase by phosphorylation in vivo. *Biochemical and Biophysical Research Communications*. http://doi.org/10.1016/j.bbrc.2013.05.028

National Research Council. (2000). Scientific Frontiers in Developmental Toxicology and Risk Assessment. In *Scientific Frontiers in Developmental Toxicology and Risk Assessment* (pp. 151–195). National Research Council.

Nelliot, A., Bond, N., & Hoshizaki, D. K. (2006). Fat-body remodeling in Drosophila melanogaster. *Genesis*, *44*, 396–400. http://doi.org/10.1002/dvg.20229

Rewitz, K. F., Yamanaka, N., & O'Connor, M. B. (2010). Steroid Hormone Inactivation Is Required during the Juvenile-Adult Transition in Drosophila. *Developmental Cell*. http://doi.org/10.1016/j.devcel.2010.10.021

Riddiford, L. M., & Truman, J. W. (1993). Hormone Receptors and the Regulation of Insect Metamorphosis'. *AMER. ZOOL*, *33*, 340–347.

Riechmann, V., Rehorn, K. P., Reuter, R., & Leptin, M. (1998). The genetic control of the distinction between fat body and gonadal mesoderm in Drosophila. *Development (Cambridge, England)*, *125*(4), 713–23. Retrieved from http://www.ncbi.nlm.nih.gov/pubmed/9435291

Ruaud, A.-F., Lam, G., & Thummel, Carl, S. (2010). The Drosophila nuclear

receptors DHR3 and BFTZ-F1 control overlapping developmental responses in late embryos. *Development*, *137*, 123–131. http://doi.org/10.1242/dev.042036

Rusten, T. E., Lindmo, K., Juhász, G., Sass, M., Seglen, P. O., Brech, A., & Stenmark, H. (2004). Programmed autophagy in the Drosophila fat body is induced by ecdysone through regulation of the PI3K Pathway. *Developmental Cell*, *7*, 179–192. http://doi.org/10.1016/j.devcel.2004.07.005

Sabino, D., Brown, N. H., & Basto, R. (2010). Drosophila Ajuba is not an Aurora-A activator but is required to maintain Aurora-A at the centrosome. *Journal of Cell Science* , *124*, 1156–1166.

Sapiro, A. L., Ihry, R. J., Buhr, D. L., Konieczko, K. M., Ives, S. M., Engstrom, A. K., … Bashirullah, A. (2013). Rapid Recombination Mapping for High-Throughput Genetic Screens in Drosophila. *G3. Genes/ Genomes/ Genetics*, *3*, 2313–2319.

Smirnova, T., Bonapace, L., Macdonald, G., Kondo, S., Ebersbach, H., Fayard, B., … Hynes, N. E. (2016). Serpin E2 promotes breast cancer metastasis by remodeling the tumor matrix and polarizing tumor associated macrophages.

Son, D., & Harijan, A. (2014). Overview of surgical scar prevention and management. *Journal of Korean Medical Science*, *29*, 751–757. http://doi.org/10.3346/jkms.2014.29.6.751

Tiede, S. L., Wassenberg, M., Christ, K., Schermuly, R. T., Seeger, W., Grimminger, F., … Gall, H. (2016). Biomarkers of tissue remodeling predict survival in patients with pulmonary hypertension. *International Journal of Cardiology*, *223*, 821–826. http://doi.org/10.1016/j.ijcard.2016.08.240

Tyler, M. (2000). Developmental Biology, A Guide for Experimental Study. In *Developmental Biology, A Guide for Experimental Study* (Second edi). Sunderland, MA: Sinauer Associates, Inc.

Walchessen, P. (2016). A Genetic Screen for Genes Involved in Tissue Remodeling.

Wang, H., Somers, G. W., Bashirullah, A., Heberlein, U., Yu, F., & Chia, W. (2006). Aurora-A acts as a tumor suppressor and regulates self-renewal of Drosophila neuroblasts. *Genes and Development*. http://doi.org/10.1101/gad.1487506

Wang, L., Evans, J., Andrews, H. K., Beckstead, R. B., Thummel, C. S., & Bashirullah, A. (2008). A genetic screen identifies new regulators of steroid-triggered programmed cell death in drosophila. *Genetics*. http://doi.org/10.1534/genetics.108.092478

Wei, S., Xie, Z., Filenova, E., & Brew, K. (2003). Drosophila TIMP Is a Potent Inhibitor of MMPs and TACE: Similarities in Structure and Function to TIMP-3. *Biochemistry*, *42*(42), 12200–12207. http://doi.org/10.1021/bi035358x

Weigmann, K., Klapper, R., Strasser, T., Rickert, C., Technau, G. M., Jackle, H., … Klambt, C. (2003). FlyMove: a new way to look at development of

Drosophila.
Worley, M. I., Setiawan, L., & Hariharan, I. K. (2012). Regeneration and Transdetermination in Drosophila Imaginal Discs. *Annu. Rev. Genet*, *46*, 289–310. http://doi.org/10.1146/annurev-genet-110711-155637
Zhang, Y., & Xi, Y. (2014). Fat Body Development and its Function in Energy Storage and Nutrient Sensing in Drosophila melanogaster. http://doi.org/10.4172/2157-7552.1000141